Thrombospondin-4 mediates hyperglycemia- and TGF-beta-induced inflammation in breast cancer

Santoshi Muppala[1], Roy Xiao[1,2], Jasmine Gajeton[1,2], Irene Krukovets[1], Dmitriy Verbovetskiy[1], and Olga Stenina-Adognravi[1]

[1]Department of Cardiovascular and Metabolic Sciences,

[2]Cleveland Clinic Lerner College of Medicine/CWRU,

Cleveland Clinic, Cleveland, Ohio

Short title: *TSP-4 promotes inflammation in breast cancer*

Address correspondence to:

Olga Stenina-Adognravi

Department of Molecular Cardiology, Cleveland Clinic

9500 Euclid Ave NB50-78, Cleveland, OH 44195

(216) 444-9057

stenino@ccf.org

Word count: 8,764

Figures: 7

Abstract:

Inflammation drives the growth of tumors and is an important predictor of cancer aggressiveness. CD68, a marker of tumor-associated macrophages (TAM), is routinely used as a marker to aid in prognosis and treatment choices for breast cancer.

We recently reported that thrombospondin-4 (TSP-4), a matricellular protein highly upregulated in several cancers, attracts macrophages into tissues during inflammation and promotes their pro-inflammatory polarization. Here, we report that TSP-4 mediates breast cancer inflammation and growth in mouse models in response to hyperglycemia and TGF-beta by increasing TAM infiltration and production of inflammatory signals in tumors. Analysis of breast cancers and non-cancerous tissue specimens from hyperglycemic patients revealed that levels of TSP-4, macrophage marker CD68, and TGF-beta signaling are upregulated in diabetic tissues. TSP-4 was co-localized with macrophages in cancer tissues. Bone-marrow-derived macrophages (BMDM) responded to high glucose by upregulating TGF-beta signaling and TSP-4 production and expression, as well as the expression of inflammatory markers.

We report a novel function for TSP-4 in breast cancer: regulation of TAM infiltration and inflammation. The results of our study provide new insights into regulation of cancer growth by hyperglycemia and TGF-beta and suggest TSP-4 as a potential therapeutic target.

Keywords: thrombospondin-4, macrophage, inflammation, breast cancer, matricellular proteins, extracellular matrix, tumor growth

ABBREVIATIONS

α-SMA, alpha-smooth muscle actin;

BMDM, bone marrow derived macrophages;

CD31, Clustre of differentiation 31(endothelial cell marker);

CD38, Cluster of differentiation 38 (macrophage pro-inflammatory marker);

CD68, Cluster of differentiation 68 (macrophage marker);

DMSO, dimethyl sulfoxide;

Egr2, Early growth response protein 2 (macrophage anti-inflammatory marker);

ECM, extracellular matrix;

Il-6, interleukin-6

m-CSF, macrophage colony stimulating factor;

mut TSP-4 KI, A387P mutant thrombospondin-4 KI;

OCT, OCT embedding cryoembedding Matrix;

RT, Room Temperature;

TSP-4, thrombospondin-4;

Thbs4-/-, *thrombospondin4* knock-out;

vWF, von Willebrand factor;

WT, wild type.

Introduction

Cancer growth depends on the interplay between the cancer cells and the tumor microenvironment. Tumor inflammation is modulated by the infiltration of immune cells and is closely associated with the tumor aggressiveness and metastasis (1). Activated cancer and vascular cells produce chemoattractants and pro-inflammatory signals to recruit inflammatory cells from blood. The accumulation of inflammatory cells in a tumor is an important prognostic index that has been successfully used to evaluate the aggressiveness of cancer in conjunction with other indexes describing the proliferation rate of cancer cells and their migratory potential. For example, one of the 12 markers evaluated in Oncotype DX (a test used to predict the aggressiveness of breast cancer and to make therapeutic decisions) is CD68, a marker of macrophages (2, 3).

The composition of the extracellular matrix (ECM) regulates recruitment of immune cells and their interactions with other cell types in a tumor. In recent years, the role of ECM, and of matricellular proteins specifically, in regulation of inflammatory cell functions attracted more attention (4-17). Thrombospondins (TSP), typical matricellular proteins that are not structural but regulate cell-ECM and cell-cell interactions, belong to a protein family that consists of five distinct members with distinct properties and roles in inflammation (18-22). While the functions of TSP-1 in regulation of inflammation have been somewhat examined, the roles for other TSPs are unknown. TSP4 is especially interesting as a potential regulator of inflammation, due to its highly upregulated levels in several conditions linked to inflammation, including coronary artery disease, heart failure, and cancers (13, 23-42). Indeed, we found that TSP-4 regulates cancer growth (26, 43) and promotes pro-inflammatory polarization of macrophages (15), in addition to regulation of the blood and

vascular cells adhesion, migration, and activation (13, 15, 16). However, the role of TSP-4 in regulation of cancer inflammation and infiltration of tumors with macrophages remained unknown. Here, we report that TSP-4 regulates cancer inflammation by increasing tumor infiltration with tumor-associated macrophages (TAM) and the levels of pro-inflammatory markers.

A rapidly-growing body of evidence connects hyperglycemia, insulin resistance, and glucose intolerance with cancer risk and progression (44-66). Diabetes, pre-diabetes, and metabolic syndrome are associated with chronic inflammation (67-70), and high glucose promotes pro-inflammatory polarization of macrophages (71-74) *in vitro*. To understand the role of TSP-4 as a mediator of hyperglycemia-induced cancer inflammation, we examined TSP-4 levels in breast cancer xenografts in mouse models of hyperglycemia and in the breast cancer tissues of hyperglycemic patients, as well as the effects of high glucose on cultured macrophages.

TGF-beta is a major regulator of tissue remodeling and inflammation and the main regulator of ECM production (75, 76), a function critical in many pathological conditions, including organ fibrosis and cancer (77-84). As a cytokine with well-studied receptors and intracellular signaling, TGF-beta and the pathways it activates are attractive therapeutic targets. However, TGF-beta has cell- and process-specific effects that are sometimes distinct and even opposite, depending on a stage and localization of a process (so-called “TGF-beta paradox)(82). In cancer, TGF-beta suppresses the growth of tumor at the early stages by inducing apoptosis and cell cycle arrest in cancer cells and by supporting cell differentiation. However, at the later stages associated with increased inflammation and angiogenesis, TGF-β promotes tumor growth and metastasis by

modulating the tumor microenvironment. We found that TGF-beta is a potent inducer of TSP-4 production in endothelial cells and macrophages (15, 43). Thus, one of the goals of the current report was to demonstrate the role of TSP-4 as a process-specific mediator of TGF-beta effects on cancer inflammation.

Our report demonstrates the effect of TSP-4 on cancer inflammation and the role of TSP-4 as a mediator of the effects of hyperglycemia and TGF-beta, two recognized drivers of cancer inflammation, growth, and metastasis with incompletely understood mechanisms of action.

Results

Increased TSP-4 expression in breast cancer tumors of hyperglycemic animals

Two mouse models of hyperglycemia, STZ-treated WT C57BL/6 mice (model of type 1 diabetes) and *Lepr*$^{db/db}$ (genetic model of type 2 diabetes) were used to examine TSP-4 expression and protein levels in EMT6 mouse breast cancer xenografts.

TSP-4 expression was significantly upregulated in tumors of both mouse models (Fig.1A and B): in STZ-treated mice, TSP-4 mRNA levels measured by RealTme RT-PCR increased from 6.9±2.98 to 111124.9±31134.7, $p = 0.00039$ in response to hyperglycemia; in *Lepr*$^{db/db}$ mice, the increase in mRNA was more modest but statistically significant, from 1.26±0.16 to 2.15±0.35, $p = 0.033$.

Increased inflammation in EMT6 mouse breast cancer of hyperglycemic mice

EMT6 cells were injected into the mammary fat pad of wild type (WT) mice treated with streptozotocin (STZ) to induce hyperglycemia (a mouse model of type 1 insulin-dependent diabetes) and normoglycemic mice injected with citric buffer (control mice) as described in Methods. RNA was purified from the tumors, and levels of mRNA of thrombospondin-4 (TSP-4), interleukin-6 (Il-6), macrophage chemoattractant protein (MCP-1, Ccl2), TNF-alpha, a macrophage marker CD68, a marker of pro-inflammatory macrophages CD38, and a marker of tissue-repair macrophages Egr2 were measured by RealTime RT-PCR (Fig.1A). The levels of all markers were significantly increased indicating a higher level of inflammation and increased TAM infiltration in tumors of

hyperglycemic animals: Il-6 mRNA levels were increased from 16±6.2 to 532±93.2, p = 4.7E-07; MCP-1 mRNA levels from 18.61±7.57 to 310±90, p = 0.0013; TNF-alpha mRNA from 8.12±2.9 to 48.5±13.2, p = 0.002; CD68 mRNA from 3.31±1.24 to 187.77±32, p = 1.18E-07; CD38 mRNA from 5.28±1.8 to 88.64±21.7, p = 2.8E-08. *Egr2* mRNA levels were also upregulated from 1.79±0.51 to 87.42±22.1, p = 0.0001 suggesting that tissue repair TAM have been recruited into tumors along with pro-inflammatory TAM.

Identical experiment was performed in hyperglycemic *Lepr*$^{db/db}$ mice (a genetic mouse model of type 2 non-insulin-dependent diabetes) and corresponding control normoglycemic heterozygous mice (Fig.1B). All inflammation and macrophage markers were upregulated in hyperglycemic *Lepr*$^{db/db}$ mice: Il-6 mRNA levels were increased from 2.09±0.2 to 9.89±0.6, p = 0.008; MCP-1 mRNA levels from 4.13±1.4 to 2429.8±862.6, p = 0.0044; TNF-alpha mRNA levels from 2.55±0.73 to 1046.1±544.8, p = 0.032; CD68 from 2.06±0.52 to 23.84±8.86, p = 0.01; CD38 mRNA from 2.50±0.63 to 6.73±0.87, p = 0.009; *Egr2* mRNA from 1.07±0.09 to 2.47±0.22, p = 1.65E-06.

Increased TSP-4 expression and protein levels in breast cancer tumors of hyperglycemic mice and patients

EMT6 tumors from hyperglycemic mice were stained with anti-TSP-4 antibody to examine localization of TSP-4 in tumors and the levels of TSP-4 proteins.

In hyperglycemic STZ-treated mice, immunofluorescence detected increased levels of TSP-4 (Fig.2A, middle panel), and co-staining with anti-CD68 antibody against

macrophage marker revealed that CD68 levels are increased in tumors from hyperglycemic mice. TSP-4 was co-localized with TAM.

Similarly, when breast cancer tissue specimens from hyperglycemic (HbAc1>7) and normoglycemic (HbAc1<6) patients were examined, most TSP-4 was associated with macrophages (Fig.2B), although co-staining with a marker of endothelial cells (EC) vWF was also detected.

Immunohistochemistry was used to detect and quantify the levels of TSP-4 protein in patients' and mouse breast cancer tumors (Fig.3A, right panel and 3B, bottom left panel). TSP-4 protein levels were higher in breast cancer tissue as compared to adjacent non-cancerous tissue and in both the cancerous and non-cancerous normal breast tissues of diabetic patients (7.01±0.38 % of total area of a section in tumor vs 3.32±0.41 % in non-cancerous in hyperglycemic patient, $p = 0.02$ and 4.73±0.21 % in tumor vs 1.03±0.20 % in non-cancerous in normoglycemic patients, $p = 0.03$).

In STZ-treated mice, TSP-4 protein levels in EMT6 tumors were increased from 0.27±0.04 % of total area of a section in normoglycemic mice to 0.61±0.11 % in hyperglycemic mice, $p = 0.007$ (Fig.3B, bottom left panel).

Increased TAM infiltration in breast cancer tumors of hyperglycemic animals and patients

mRNA of a macrophage marker CD68 was upregulated in EMT6 tumors of STZ-treated and *Lepr*$^{db/db}$ mice (Fig.1A and B) suggesting increased number of macrophages in cancer xenografts grown in hyperglycemic mice.

Increased number of macrophages in tumors of hyperglycemic animals was detected by immunofluorescence and immunohistochemistry with anti-CD68 antibody (Fig.2A and 3B, upper left panel): the area stained with anti-CD68 increased from 1.70±0.19 % of total area of a section in control normoglycemic mice to 3.51±0.62 % in STZ-treated hyperglycemic mice, $p = 0.005$. Immunohistochemistry with MOMA-2, another antibody recognizing mouse macrophages, supported the data obtained with anti-CD68 antibody: area stained with MOMA-2 antibody significantly increased in tumors from hyperglycemic mice (Fig.3B, bottom right panel)

CD68 protein levels were higher in breast cancer tissue as compared to adjacent non-cancerous tissue (stained area 3.63±0.20 % of total section area in tumor vs 2.2±0.27 % in non-cancerous in hyperglycemic patient, $p = 0.04$ and 2.26±0.10 % in tumor vs 1.01±0.20 % in non-cancerous in normoglycemic patients, $p = 0.01$) (Fig.3A, left panel). The levels of CD68 were significantly higher in diabetic tissues, in both the cancerous and the non-cancerous adjacent tissue.

Increased TGF-beta signaling in breast cancer tumors of hyperglycemic animals and patients

Previously, we reported that TGF-beta induces TSP-4 production (15, 43). TGF-beta is also implicated in breast cancer growth (43, 85, 86). Therefore, we examined TGF-beta signaling in breast cancer tumors from hyperglycemic mice and patients by staining the tissues with anti-phosphorylated Smad3 (p-Smad3), a TGF-beta signaling intracellular protein responsible for TSP-4 upregulation by TGF-beta (43).

Similarly to the levels of TSP-4 and CD68, p-Smad3 protein levels were higher in breast cancer tissue as compared to adjacent non-cancerous tissue and in all breast tissues of diabetic patients as compared to non-diabetic patients (stained area of 0.17±0.04 % of the total sections area in tumor vs 0.09±0.045 % in non-cancerous in hyperglycemic patients, $p = 0.05$ and 0.07±0.005 % in tumor vs 0.02±0.001 % in non-cancerous in normoglycemic patients, $p = 0.006$) (Fig.3A, right panel).

EMT6 tumors from control normoglycemic mice had only traces of staining for p-Smad3, but a significant increase in stained area was detected in tumors from the hyperglycemic STZ-treated mice: (0.05±0.01 % of total area to 0.6±0.006 %, $p = 0.02$) (Fig.3B, upper right panel).

Effect of high glucose on TSP-4 production and TGF-beta signaling by cultured bone-marrow-derived macrophages (BMDM)

Because most of TSP-4 protein was co-localized with TAM in tumors, we isolated bone-marrow-derived macrophages (BMDM) from WT, *Thbs4*$^{-/-}$ (TSP-4 KO mice), and P387-TSP-4 KI mice expressing a mutant form of TSP-4 that is more active in all cellular interactions (14-16, 26, 43, 87-89). Cultured BMDB were incubated in low (5 mM) D-glucose or high (30 mM) D-glucose and stained with anti-CD68, anti-TSP-4, and anti-p-Smad3 antibodies (Fig.4).

TSP-4 levels were increased in BMDB isolated from WT mice in response to high glucose (Fig.4 A and B). TSP-4 levels were higher in cultured BMDM from P387-TSP-4-KI mice (Fig.4B), consistent with our previous observations of higher stability of the

mutant protein (88, 89). High glucose increased p-Smad3 levels but not the levels of CD68. Interestingly, the deficiency in TSP-4 (*Thbs4*$^{-/-}$, TSP-4 KO) reduced both the level of CD68 and the level of p-Smad3 (Fig.4A), while the expression of a more active P387-TSP-4 resulted in higher levels of p-Smad3 (Fig.4B), suggesting a more complex cross-talk in signaling pathways and regulation of TGF-beta signaling by TSP-4, in addition to the reported regulation of TSP-4 production by TGF-beta (15, 43).

TGF-beta increases inflammation in mouse breast cancer

Because the increased TGF-beta signaling was observed in cancers of hyperglycemic mice and patients (Fig. 3 and 4) and correlated with increased levels of TSP-4 and inflammation, we examined the effect of TGF-beta1 injections on TSP-4 and inflammation in mouse EMT6 cancer. Mice with EMT6 xenografts were injected intraperitoneally daily with 500 ng/kg TGF-beta. mRNA was extracted from the tumors at the end of the experiment, and the expression of TSP-4 and inflammation markers was examined by Real-Time RT-PCR (Fig.5A). Daily TGF-beta1 injections resulted in increased levels of TSP-4, macrophage marker CD68, and inflammation markers IL-6, Ccl2 (MCP-1), and TNF-alpha. TSP-4 mRNA levels increased from 1.62±0.54 to 5.21±1.53, $p = 0.04$, CD68 mRNA levels increased from 1.07±0.08 to 2.06±0.36, $p = 0.005$, IL-6 levels from 1.13±0.17 to 2.02±0.07, $p = 0.00013$, Ccl2 from 1.21±0.16 to 1.93±0.39, $p = 0.049$ and TNF-alpha from 1.39±0.26 to 2.45±0.52, $p = 0.040$. The levels of a marker of pro-inflammatory macrophages CD38 were increased by TGF-beta1 one injections 1.08±0.10 to 1.58±0.24, $p = 0.035$, while the levels of a marker of tissue-repair macrophages were decreased from 1.10±0.17 to 0.57±0.06, $p = 0.05$.

TSP-4 deletion reduces inflammation in mouse breast cancer

TSP-4 levels were increased by both the high glucose and the TGF-beta1 (Fig. 1-5). To understand the role of TSP-4 in cancer inflammation, EMT6 cells transduced with TSP-4 shRNA (26) were injected into WT or *Thbs4*$^{-/-}$ mice (Fig.5B). The expression of a macrophage marker CD68, Cd38, Egr2, and MCP-1 was quantified by Real-Time RT-PCR and was found to be decreased in *Thbs4*$^{-/-}$ mice, indicating that TSP-4 promotes TAM infiltration of tumors and inflammation. CD68 expression was decreased from 1.36±0.19 to 0.75±0.11, p = 0.01; Ccl2 (MCP-1) expression was decreased from 1.37±0.22 to 0.26±0.03, p = 0.0003, indicating a lower level of inflammation in the absence of TSP-4.

Effect of TSP-4 deletion on the expression of inflammatory markers by BMDM in response to high glucose

The role of TSP-4 in high-glucose-induced upregulation of inflammatory markers was tested using BMDM isolated from WT mice and from *Thbs4*$^{-/-}$ mice (Fig.6A). Deletion of TSP-4 prevented the increases in mRNA levels of macrophage marker Cd68: the levels were reduced from 1.05±0.23 to 0.55±0.06, p = 0.05, in non-stimulated *Thbs4*$^{-/-}$ BMDM and from 2.61±0.29 to 0.44±0.14, p = 0.001, in glucose-stimulated *Thbs4*$^{-/-}$ BMDM. The increase in mRNA levels of Cd38 in response to high glucose was also prevented, and the levels of mRNA of the pro-inflammatory macrophage marker Cd38 were reduced from 1.01±0.11 to 0.36±0.03, p = 0.002, in non-stimulated *Thbs4*$^{-/-}$ cells and from 1.92±0.12 to 0.11±0.02, p = 6.66651E-05, in glucose-stimulated *Thbs4*$^{-/-}$ cells. Tissue repair macrophage markers Arg1 was also increased in response to high glucose, and

this increase was also prevented by TSP-4 deletion. The increase in mRNA of another marker of tissue repair macrophage, Egr2, was also prevented in *Thbs4*$^{-/-}$ BMDM, and the levels were significantly lower in TSP-4 deficient cells: 1.01±0.09 vs 0.66±0.07, p = 0.02 in non-stimulated WT cells vs *Thbs4*$^{-/-}$ cells and 1.80±0.29 vs 0.42±0.06, p = 0.004 in glucose-stimulated WT cells vs *Thbs4*$^{-/-}$ cells. High glucose significantly increased TNF-alpha mRNA, but the increase was completely prevented in BMDM from *Thbs4*$^{-/-}$ mice, and the levels were significantly lowered (1.01±0.10 in non-stimulated WT cells vs 0.43±0.09, p = 0.006 in non-stimulated *Thbs4*$^{-/-}$ cells; and 1.61±0.05 in glucose-stimulated WT cells vs 0.62±0.12, p = 0.0008 in glucose-stimulated *Thbs4*$^{-/-}$ cells. Although the deletion of TSP-4 did not prevent upregulation of IL-6 mRNA in response to high glucose, the levels of mRNA of IL-6 were significantly lower in BMDM from *Thbs4*$^{-/-}$ mice: 1.02±0.16 vs 0.64±0.06, p = 0.04 in non-stimulated WT cells vs *Thbs4*$^{-/-}$ cells and 3.72±0.20 vs 2.28±0.29, p = 0.007 in glucose-stimulated WT cells vs *Thbs4*$^{-/-}$ cells. Similarly to Il-6 mRNA, Ccl2 (MCP-1) mRNA was still significantly upregulated in response to high glucose in *Thbs4*$^{-/-}$ cells, but the levels were lower in both non-stimulated *Thbs4*$^{-/-}$ cells and in glucose-stimulated *Thbs4*$^{-/-}$ cells as compared to WT cells (1.02±0.14 in non-stimulated WT cells vs 0.52±0.02, p = 0.01 in non-stimulated *Thbs4*$^{-/-}$ cells and 3.42±0.46 in glucose-stimulated WT cells vs 1.60±0.19, p = 0.01 in glucose-stimulated *Thbs4*$^{-/-}$ cells).

Interestingly, the levels of mRNA of Nos2, another marker of pro-inflammatory macrophages were significantly increased in *Thbs4*$^{-/-}$ BMDM independently of glucose concentration, suggesting not only a higher complexity of regulation of pro-inflammatory

TAM polarization, but also a direct glucose-independent regulation of iNOS expression by TSP-4.

Effect of TSP-4 deletion on TGF-beta induced inflammation

Previously, we reported that TSP-4 mediates the effects of TGF-beta1 on cancer angiogenesis (43). Based on our previous report and the correlation between TGF-beta, TSP-4 and inflammation that we described above, we hypothesized that TSP-4 may mediate the effects of TGF-beta1 on cancer inflammation. Deletion of TSP-4 did not effect the expression of Cd68: in BMDM from *Thbs4*$^{-/-}$ mice, Cd68 mRA level was still significantly increased in response to TGF-beta1 stimulation. The expression of Cd38 was only modesty upregulated by TGF-beta1 in WT cells (from 1.00±0.06 to 1.22±0.23, p = 0.01), and this modest but statistically significant upregulation was prevented by TSP-4 deletion. Nos2 levels were significantly increased by TGF-beta1 in WT cells from 1.00±0.06 to 3.46±0.83, p = 0.02, p = 0.008, and the increase was completely prevented in BMDM from *Thbs4*$^{-/-}$ mice, with the levels 1.10±0.15 in TGF-beta 1-stimulated *Thbs4*$^{-/-}$ cells. Il-6 expression was upregulated two-fold by TGF-beta1, from 1.00±0.05 to 1.96±0.44, p = 0.01. Although the upregulation was still detected in BMDM from *Thbs4*$^{-/-}$ mice, from 0.35±0.01 to 0.62±0.05, p = 0.01, the levels of Il-6 mRNA in cells from *Thbs4*$^{-/-}$ mice were significantly lower in both non-stimulated cells and TGF-beta1-stimulated cells as compared to WT cells in the same condition. The modest increase in TNF-alpha expression was prevented in cells from *Thbs4*$^{-/-}$ mice. There was no effect of TSP-4 deletion on the levels of tissue repair macrophage markers Arg1 and Egr2, and it was noteworthy that the expression of Arg1 was dramatically upregulated

while Egr2 expression was decreased, consistent with the mixed pro-and anti-inflammatory effects of TGF-beta in cancer and other pathological conditions. Ccl2 (MCP-1) mRNA levels were decreased in response to TGFpbeta1 stimulation, and TSP-4 depetion had no effect on the expression of Ccl2.

Deletion of TSP-4 significantly decreased the levels of CD68 protein in EMT6 tumors in *Thbs4*$^{-/-}$ mice (from 0.93±0.25 vs 0.35±0.09, p = 0.0006) and the elvels were also decreased in Thbs4-/- mice injected with TGF-beta1 as compared to WT mice (from 10.67±4.78 to 3.23±1.32, p = 0.006) (Fig.7A).

TSP-4 does not mediate the effects of TGF-beta on collagen production

To investigate whether TSP-4 mediates other effects of TGF-beta1 in breast cancer tumors, in addition to regulation of angiogenesis and inflammation, we examined collagen I and IV (Col I and IV) levels in tumors grown in WT and *Thbs4*$^{-/-}$ mice (Fig.7B). Both Col I and Col IV levels were increased in *Thbs4*$^{-/-}$ mice, consistent with our previous observation of suppression of collagen production by TSP-4 (90). TGF-beta1 decreased the level of Col I in a TSP-4-dependent manner: the decrease was completely prevented in *Thbs4*$^{-/-}$ mice. The levels of Col IV were decreased in response to TGF-beta1 injections independently of the presence or the absence of TSP-4, suggesting that TSP-4 does not mediate the effect of TGF-beta on collagen IV production or turnover.

Discussion

TSP-4 is one of the top upregulated genes in several cancers, including the breast cancer (40-42). Using *Thbs4*$^{-/-}$ mice, we demonstrated that TSP-4 deletion prevents the growth of cancer and mediates some of the effects of TGF-beta1 in tumors (43). Cancer angiogenesis that is stimulated by the growing cancer and supports the tumor growth was TSP-4-dependent.

Tumor inflammation is an important marker of cancer aggressiveness and is defined by tumor microenvironment, including the composition of the tumor ECM. We recently reported that TSP-4 promotes the accumulation of macrophages in tissues and regulates their pro-inflammatory polarization, adhesion, and migration (13, 15, 16). Taking in the account the dramatically increased levels of TSP-4 in some cancers, its effects on tumor growth, and its role in regulation of macrophage polarization and function, in this work, we investigated whether TSP-4 regulates cancer inflammation.

We chose two well-known regulators of ECM production, inflammation, and cancer growth – hyperglycemia (44-47, 49, 91) and TGF-beta (43, 85, 86). Both are known to regulate the remodeling of tissues, and of cancer microenvironment specifically. Both have poorly understood effects on cancer growth and ECM.

We found that TGF-beta signaling (the phospho-SMAD3 level) is upregulated in breast cancer tissues of hyperglycemic mice and patients, linking the two stimuli, hyperglycemia and TGF-beta, together. Both the hyperglycemia and TGF-beta stimulations *in vivo* and in cultured BMDM resulted in increased expression and protein

levels of TSP-4. We have reported that TGF-beta induces upregulation of TSP-4 in endothelial cells and macrophages, but the increased TSP-4 production in response to high glucose is a new observation. Whether this is a direct effect of high glucose or the effect on TSP-4 production is mediated by TGF-beta is yet unknown. Differential effects of the two stimuli on cultured BMDM and differential roles of TSP-4 in the effects of high glucose and TGF-beta1 on BMDM suggest that glucose effects TSP-4 levels in TGF-beta-independent manner, at least partially.

Several markers of inflammation were examined in breast cancer tissues of hyperglycemic mice and patients: inflammatory cytokines Il-6, Ccl2 (MCP-1) and TNF-alpha, as well as a macrophage marker CD68, markers of pro-inflammatory macrophages CD38 and iNOS, and markers of tissue repair anti-inflammatory macrophages Egr2 and Arg1. Whether hyperglycemia was the result of streptozotocin (STZ) treatment (type 1 mouse insulin-dependent diabetes model, in which pancreatic islet cells are destroyed and insulin is no longer produced) or resulted from a genetic mutation in the leptin receptor leading to insulin resistance and hyperglycemia (*Lepr*$^{db/db}$ mice, type 2 non-insulin-dependent diabetes model), increased infiltration of macrophages and increased levels of all inflammatory markers were detected, documenting higher cancer inflammation in tumors of hyperglycemic mice. Similarly, higher macrophage infiltration of tumors and adjacent non-cancerous tissues was observed in specimens of hyperglycemic patients, parallel to the increased levels of TSP-4 in these specimens. We have previously reported that TSP-4 can be produced by endothelial, smooth muscle cells, and by macrophages (13, 15, 16, 26, 35, 89). Most of TSP-4 in tumors was associated with macrophages, and only a small portion was co-

localized with endothelial cells, suggesting that macrophages are the main or at least the major producers of TSP-4 in tumors.

Using BMDM isolated from WT mice, *Thbs4*$^{-/-}$ mice, and mice expressing a more active and more stable form of the protein P387-TSP-4 (*P387-TSP4-KI*), we tested the effect of high glucose on the levels of TSP-4 and TGF-beta signaling. High glucose increased the production of TSP-4 by BMDM in WT cells, and the levels of phospho-Smad3 were also increased by the treatment. Interestingly, in the absence of TSP-4, the effect of high glucose on the levels of phospho-Smad3 was almost completely lost, and the glucose-stimulated cells expressing P387-TSP-4 also had a lower levels of phospho-Smad3 than unstimulated cells. From our previous work, we know that Smad3 mediates, at least partially, increased levels of TSP-4 in response to TGF-beta1 (43) and that TSP-4, in turn, regulates TGF-beta signaling in an apparent feed-back pathway (90). The new observations of reduced phospho-Smad3 levels in both the cells deficient in TSP-4 and expressing a more active form of TSP-4 suggest even more complex relationships between TSP-4 and TGF-beta signaling.

The deletion of TSP-4 in mice (*Thbs4*$^{-/-}$ mice) and EMT6 cancer cells [EMT6 stably transduced with TSP-4 shRNA] resulted in significantly reduced expression of macrophage marker CD68, pro-inflammatory macrophage marker CD38, CCl2 (MCP-1), but not a marker of tissue repair macrophages Egr2 in EMT6 mouse xenografts, consistent with regulation of macrophage infiltration and upregulation of inflammation by TSP-4 (13, 15, 16).

To prove the role of TSP-4 as a mediator of proinflammatory effects of high glucose and TGF-beta in macrophages, cultured BMDM from WT and *Thbs4*$^{-/-}$ mice were stimulated with high glucose or with TGF-beta1. Although the deletion of TSP-4 clearly resulted in lower production of inflammatory markers by the cultured BMDM, the effects were distinct and specific, suggesting that the effects of high glucose may not be mediated by TGF-beta but rather that the two stimuli activate some non-overlapping pro-inflammatory pathways. Increased expression of CD68 in response to high glucose was completely prevented by TSP-4 deletion, but the increase in response to TGF-beta was not. Increase in iNOS mRNA levels in response to TGF-beta1 was completely prevented in the absence of TSP-4, while TSP-4 deletion resulted in further increase in iNOS expression in response to high glucose. The effects of TSP-4 knock-out on the expression of markers of the tissue repair macrophages were also distinct: in the absence of TSP-4, increases in both Arg1 and Egr2 expression in response to high glucose were prevented, but the deletion did not affect the change in the expression of either marker in response to TGF-beta1. Remarkably, the effect on the expression of Ccl2 (MCP-1) in BMDM was opposite in cells stimulated with high glucose and TGF-beta: high glucose increased it, but TGF-beta1 decreased the expression. The effects on the expression of a marker of pro-inflammatory macrophages CD38, Il-6, and TNF-alpha were similar: both the high glucose and TGF-beta1 increased the expression, and the deletion of TSP-4 prevented the increases. Thus, TSP-4 mediated the pro-inflammatory effects of both high glucose and TGF-beta in cultured macrophages, although the regulation by both stimuli was different in cell culture than in *in vivo* tumors, where there was more consistency in the direction of the effects, suggesting that the

inflammation patterns in tumors are not defined by macrophages only, but other cell types contribute to the pro-inflammatory environment as well.

In vivo in EMT6 xenografts, TGF-beta1 injections increased macrophage infiltration as was detected by the staining of the tumor sections with anti-CD68 antibody. The macrophage infiltration was decreased in tumors of *Thbs4*$^{-/-}$ mice, demonstrating that TSP-4 mediates the regulation of cancer inflammation in response to TGF-beta1.

Stiffening of the tumor ECM due to increased levels of collagen and fibronectin is an important event in cancer progression (92). Although TSP-4 mediates TGF-beta1 effects on cancer growth (ref), angiogenesis (ref), and inflammation, TSP-4 involvement is process-specific. When we examined the effects of TSP-4 deletion on regulation of collagen depositions in response to TGF-beta1, we found that levels of collagen IV are regulated by TGF-beta in TSP-4-independent manner: TGF-beta1 downregulated collagen IV depositions in both the WT and *Thbs4*$^{-/-}$ mice. The levels of collagen I were downregulated in tumors of WT mice, but TSP-4 deletion prevented the effect. Consistent with our previous observation of downregulation of collagen production by cultured dermal fibroblasts by TSP-4 (90), both collagen I and collagen IV levels were upregulated in tumors of *Thbs4*$^{-/-}$ mice. Distinct effects of TSP-4 deletion suggest that the role of TSP-4 in TGF-beta-induced is process-specific. TSP-4 mediates the pro-inflammatory effects of high glucose and TGF-beta and some effects of TGF-beta on ECM production, but the changes mediated by TSP-4 are different for each stimulus and function.

Our work describes a role for TSP-4 in cancer inflammation and identifies the pathways, in which increased levels of TSP-4 in tumor plays an important role and promotes cancer growth by increasing cancer inflammation.

Methods

Patient's breast cancer and adjacent normal tissue specimens were obtained from the Cleveland Clinic Tissue Bank. The work was approved by the Cleveland Clinic Institutional Review Board. All patients were female. Patients with HbAc1 < 6 were considered normoglycemic; patients with HbAc1 > 7 or documented diabetes diagnosis were considered hyperglycemic.

Animals. Mice were of the C57BL/6 background. Both genders were used (there were no gender-specific differences). *Thbs4*$^{-/-}$ and P387-TSP4-KI mice were described previously (15, 16). Control wild-type (WT) mice were from the same mouse colony as the knock-out and knock-in mice. Animals were housed in the AAALAC- approved animal facilities of the Cleveland Clinic. Animal procedures were approved by the IACUC and were in agreement with the NIH Guide for Animal Use. Ketamine (80mg/kg)/Xylazine (15mg/kg) was used for anesthesia to immobilize the mice for subcutaneous injections. *Lepr*$^{db/db}$ (animal model of type 2, non–insulin-dependent, diabetes), *Lepr*$^{db/+}$ (corresponding control mice), and wild-type C57BL/6 were purchased from The Jackson Laboratory (Bar Harbor, ME, USA).

Induction of hyperglycemia in mice. Hyperglycemia was induced by streptozotocin (STZ) injections according to the Jackson Laboratory protocol and as described in our publication (93, 94). Citric buffer was injected to control normoglycemic mice. One week after the first STZ injection, blood glucose was measured with an Alphatrak glucometer and blood glucose strips for mice and rats from Abbott (Abbott Park, IL, USA), and mice

with levels ≥250 mg/dl were included in the experiments. STZ-induced hyperglycemia is an animal model of type 1, insulin-dependent diabetes.

EMT6 mouse breast cancer xenografts. Fifteen- to sixteen-week-old mice were anesthetized by IP injection of Ketamine (80mg/kg)/Xylazine (15mg/kg) mixture. Mice were injected in the mammary fat pad with 1.5×10^6 EMT6 cells (ATCC) in 100 µl of saline. TGF-β1 (500ng/kg) injections were given IP daily for 14 days. Tumors were harvested ion day 14 and frozen in OCT in liquid nitrogen. 10 µm sections were stained using specific antibodies.

Isolation of Bone Marrow Derived Macrophages (BMDM) and cell culture. Bone marrow derived macrophages (BMDM) were isolated from WT and *TSP-4*$^{-/-}$ mice using M-CSF (14-8983-62, ThermoFisher) with DMEM/F12 for 5 days and treated them either with D-Glucose (30mM) or TGF-beta (10ng/ml) for 6h and 24h respectively along with proper controls were directly used for isolation of RNA and immunofluorescence experiments. BMDM were supplemented with low glucose and 1% serum 24h before the treatment with D-Glucose.

Quantitative real-time RT-PCR analysis. Total RNA was extracted using TRIzol Reagent (#15596026, ThermoFisher) followed by cDNA synthesis using SuperScript™ First-Strand Synthesis System (#11904018, ThermoFisher). Taqman fast Master mix (#4444557, ThermoFisher). The TaqMan® probe for *Thbs4* (Assay ID# Mm03003598_s1, ThermoFisher), *CD68* (Assay ID# Mm03047343_m1, ThermoFisher), *CD38* (Assay ID# Mm01220906_m1, ThermoFisher), *Egr2* (Assay ID# Mm00456650_m1, ThermoFisher), IL-6 (Assay ID# Mm00446191_m1, ThermoFisher),

TNF-alpha (Assay ID# Mm00443258_m1, ThermoFisher), MCP-1 (Assay ID# Mm00441242_m1, ThermoFisher) *Nos2* (Assay ID# Mm00440502_m1, ThermoFisher), *Arg1* (Assay ID# Mm00475988_m1, ThermoFisher) were used for detecting respective genes expressions with Stx5a (Assay ID# Mm00502335_m1, ThermoFisher)) and *ACTB* (Assay ID# Mm04394036_g1, ThermoFisher), GAPDH (Assay ID# Mm_99999915_m1) , RN18s (Assay ID# Mm03928990_g1, ThermoFisher) were used as housekeeping gene controls.

Immunohistochemistry, immunofluorescence, confocal imaging and quantification of macrophage markers. Sections of STZ treated mice tumors were stained with primary rat anti-mouse CD68 antibody (MCA1957B, Bio-Rad), goat anti-human TSP-4 (AF2390, R&D Systems) and pSmad3 (Phospho-S423+S425, EP8234, ab52903, Abcam). Sections of human diabetic breast cancer tumors were stained with anti-pSMAD3 (Phospho-S423+S425, EP8234, ab52903, Abcam), mouse anti-human CD68 (Dako) and goat anti-human TSP-4 (AF2390, R&D Systems) using Vecta Stain ABC Kit (PK-6104, PK-6102, PK-6105 Vector). Visualization after staining with the antibodies was performed using a high-resolution slide scanner (Leica SCN400FL, Leica microsystems, GmbH, Wetzlar, Germany) at 20 × magnification. High-resolution images of the whole section were generated and quantified to determine the percentage of the stained area using Adobe photoshop CS6 (Media Cybernetics). The person performing quantification was blinded to the assignment of animals between groups. For immunofluorescence, Collagen I (Ab6308, Abcam) and Collagen IV (Ab6586, Abcam), pSMAD3 (Phospho-S423+S425, EP8234, ab52903, Abcam), rat anti-mouse CD68 (MCA1957B, Bio-Rad), goat anti-human TSP-4 (AF2390, R&D Systems), monoclonal

mouse anti-human alpha smooth muscle actin (M0851, Dako), monoclonal mouse anti-human CD68 (M0814, Dako), rabbit anti-human vWF antibody (A0082, Dako), were used with corresponding secondary antibodies. Secondary antibodies were anti-goat NL557 conjugated donkey IgG (NL001 R&D Systems), goat polyclonal antibody to rat IgG Alexa Fluor 488 (ab150161, abcam), anti-mouse IgG NL493 conjugated donkey IgG (NL009, R&D Systems), Alexa Fluor™647 F(ab')2 fragment of goat anti-mouse IgG(H+L) (A21237, Invitrogen) and Alexa Fluor™647 chicken anti-rabbit IgG (H+L) (A21443, Invitrogen). Images were taken at a high-resolution confocal microscope (Leica DM 2500). 4% horse serum (S-2000, Vector) was used for blocking for 1 hour at RT and primary antibody incubation for overnight at 4 °C and secondary antibody incubation for 1 hour at RT.

Statistical analysis. Analyses of the data were performed using Sigma Plot Software (Systat Software, San Jose, CA, USA): Student's t-test and one-way ANOVA were used to determine the significance of parametric data, and Wilcoxon rank sum test was used for nonparametric data. The significance level was set at $p=0.05$. The data are presented as mean±S.E.M.

Author contributions

Santoshi Muppala: designed and performed experiments, collected analyzed the data, prepared figures and a draft of the manuscript.

Roy Xiao: designed and performed experiments, collected analyzed the data, prepared figures and a draft of the manuscript.

Jasmine Gajeton: designed and performed experiments, collected analyzed the data, prepared figures, obtained funds to support a part of the work.

Irene Krukovets: designed and performed experiments, collected analyzed the data, prepared figures.

Dmitriy Verbovetskiy: designed and performed experiments, collected analyzed the data, prepared figures.

Olga Stenina-Adognravi: secured funds to support the work and the approvals by IACUC and IRB, provided oversight of all activities, designed experiments, analyzed the data, prepared figures and the final version of the manuscript.

Acknowledgments

This work was supported by the National Institutes of Health awards R01 HL117216 and R01 CA177771 and by the American Heart Association award 17PRE33660475.

Figure Legends

Figure 1. Increased expression of inflammatory markers in breast cancer tumors in hyperglycemia mice. EMT6 mouse breast cancer cells were injected into mammary fat pad of hyperglycemic WT STZ-treated **(A)** n=10, mean ± S.E.M and *Lepr*$^{db/db}$ **(B)** mice as described in methods, and mRNA levels of TSP-4, MCP-1, TNF-alpha, macrophage marker Cd68, inflammatory macrophage marker Cd38, and tissue repair macrophage marker Egr2 were measured by RealTime RT-PCR in tumors. n=5, mean ± S.E.M.

Figure 2. Increased TSP-4 levels and inflammation breast cancers of hyperglycemic mice and patients. Immunofluorescent staining of CD68, TSP-4 and vWF, (red: *Thbs4* stained with anti–TSP-4, green: macrophages stained with anti-CD68 antibody, magenta: vWF stained with anti-vWF; blue: nuclei stained with DAPI). **A:** Immunostaining of EMT6 tumors harvested from normoglycemic control (left panel) and hyperglycemic (STZ-treated, right panel) WT C57BL/6 mice; **B:** Immunostaining of tumors and adjacent non-cancerous tissues from normoglycemic (HbAc1<6) and hyperglycemic (HbAc1>7) patients. Scale bar = 10 μM.

Figure 3. Quantification of the levels of TSP-4, macrophage marker CD68, and phosphorylated pSmad3 in tumors of hyperglycemic patients and mice. TSP-4, CD68, and pSmad3 were stained with corresponding antibodies as described in Methods. **A:** Immunohistochemistry images and quantification of protein levels in tumors (cancer) and adjacent non-cancerous tissue (Normal) from diabetic (Hyperglycemic) and non-diabetic (Hyperglycemic) patients. **B:** Immunohistochemistry

images and quantification of protein levels in tumors from hyperglycemic (STZ) and normoglycemic (Control) mice. Mean ± S.E.M; scale bar = 20 μM.

Figure 4. TSP-4 mediates the effect of high glucose on TGF-beta signaling in cultured bone-marrow-derived macrophages (BMDM). TSP-4, macrophage marker Cd68, and pSMAD3 were visualized in cultured BMDM using corresponding antibodies. BMDM from WT mice, *Thbs4*$^{-/-}$ mice (TSP-4 KO, **A**) and mice expressing more active form of TSP-4, P387 TSP-4 (TSP-4 KI, **B**) were stimulated with 25 mM L- or D- glucose for 24 h. Blue: nuclei, DAPI; green: anti-Cd68; red: anti-TSP-4; magenta: anti-phospho-Smad3. Scale bar = 30 μM.

Figure 5. TGF-beta1 and TSP-4 increase inflammation in mouse breast cancer. A: Expression of TSP-4, IL-6, MCP-1, TNF-alpha, macrophage marker Cd68, pro-inflammatory macrophage marker Cd38, and tissue repair macrophage marker Egr2 was measured in EMT6 mouse breast cancers of mice injected with TGF-beta as described in Methods. **B:** Cd68, Cd38, Egr2, and MCP-1 mRNA levels were measured in EMT6 mouse breast cancers grown in WT and Thbs4-/- mice. RealTime RT-PCR, mean± S.E.M.

Figure 6. TSP-4 mediates the effects of high glucose and TGF-beta1 on the levels of inflammatory markers in cultured BMDM. Cultured BMDM from WT and *Thbs4*$^{-/-}$ (TSP-4 KO) mice were stimulated with 25 mM D-glucose for (A) or 10ng/ml of TGF-beta1 (B) for 24 h, n=10; mean± S.E.M; *$p<0.05$ in comparison to control of the same genotype; $^{\#}p<0.05$ in comparison to the same experimental condition in different genotype.

Figure 7. TSP-4 mediates macrophage accumulation and collagen production in breast cancer in response to TGF-beta1. A: CD68 was visualized in EMT6 tumors of WT and *Thbs4*$^{-/-}$ mice injected with TGF-beta1, and the stained area was quantified as described in Methods. Immunohistochemistry; mean± S.E.M; *$p<0.05$ as compared to corresponding no treatment control, $^{\#}p<0.05$ as compared to the same treatment in different genotype. **B:** TSP-4 (red), nuclei (blue), collagen I (green) and collagen IV (magenta) were visualized using corresponding antibodies. Immunofluorescence, scale bar = 50 μM.

References

1. Yang L, and Lin PC. Mechanisms that drive inflammatory tumor microenvironment, tumor heterogeneity, and metastatic progression. *Semin Cancer Biol.* 2017;47:185-95.

2. Medrek C, Ponten F, Jirstrom K, and Leandersson K. The presence of tumor associated macrophages in tumor stroma as a prognostic marker for breast cancer patients. *BMC Cancer.* 2012;12:306.

3. Barcenas CH, Raghavendra A, Sinha AK, Syed MP, Hsu L, Patangan MG, Jr., et al. Outcomes in patients with early-stage breast cancer who underwent a 21-gene expression assay. *Cancer.* 2017;123(13):2422-31.

4. Jia Y, Zhong F, Jiang S, Guo Q, Jin H, Wang F, et al. Periostin in chronic liver diseases: Current research and future perspectives. *Life Sci.* 2019;226:91-7.

5. Sikkema AH, Stoffels JMJ, Wang P, Basedow FJ, Bulsink R, Bajramovic JJ, et al. Fibronectin aggregates promote features of a classically and alternatively activated phenotype in macrophages. *J Neuroinflammation.* 2018;15(1):218.

6. Mirzoeva S, Tong X, Bridgeman BB, Plebanek MP, and Volpert OV. Apigenin Inhibits UVB-Induced Skin Carcinogenesis: The Role of Thrombospondin-1 as an Anti-Inflammatory Factor. *Neoplasia.* 2018;20(9):930-42.

7. Xiao M, Zhang J, Chen W, and Chen W. M1-like tumor-associated macrophages activated by exosome-transferred THBS1 promote malignant migration in oral squamous cell carcinoma. *J Exp Clin Cancer Res.* 2018;37(1):143.

8. Chen J, Luo Y, Zhou Y, Qin S, Qiu Y, Cui R, et al. Promotion of Tumor Growth by ADAMTS4 in Colorectal Cancer: Focused on Macrophages. *Cell Physiol Biochem.* 2018;46(4):1693-703.

9. Li Y, Qi X, Tong X, and Wang S. Thrombospondin 1 activates the macrophage Toll-like receptor 4 pathway. *Cell Mol Immunol.* 2013;10(6):506-12.

10. Xing T, Wang Y, Ding WJ, Li YL, Hu XD, Wang C, et al. Thrombospondin-1 Production Regulates the Inflammatory Cytokine Secretion in THP-1 Cells Through NF-kappaB Signaling Pathway. *Inflammation.* 2017;40(5):1606-21.

11. Navarathna DH, Stein EV, Lessey-Morillon EC, Nayak D, Martin-Manso G, and Roberts DD. CD47 Promotes Protective Innate and Adaptive Immunity in a Mouse Model of Disseminated Candidiasis. *PLoS One.* 2015;10(5):e0128220.

12. Martin-Manso G, Navarathna DH, Galli S, Soto-Pantoja DR, Kuznetsova SA, Tsokos M, et al. Endogenous thrombospondin-1 regulates leukocyte recruitment and activation and accelerates death from systemic candidiasis. *PLoS One.* 2012;7(11):e48775.

13. Frolova EG, Pluskota E, Krukovets I, Burke T, Drumm C, Smith JD, et al. Thrombospondin-4 regulates vascular inflammation and atherogenesis. *Circ Res.* 2010;107(11):1313-25.

14. Pluskota E, Stenina OI, Krukovets I, Szpak D, Topol EJ, and Plow EF. Mechanism and effect of thrombospondin-4 polymorphisms on neutrophil function. *Blood.* 2005;106(12):3970-8.

15. Mohammed Tanjimur Rahman M, Ph.D., Santoshi Muppala, Ph.D., Jiahui Wu, Ph.D., Irene Krukovets, M.S., Dmitry Solovjev, Ph.D., Dmitriy Verbovetskiy, M.D., Edward F. Plow, Ph.D., and Olga Stenina-Adognravi, Ph.D. . Thrombospondin-4 promotes pro-inflammatory phenotype and apoptosis in macrophages. *Cell Death & Disease.* 2019;in press.

16. Santoshi Muppala PD, Mohammed Tanjimur Rahman, Ph.D. , Irene Krukovets, M.S. , Dmitriy Verbovetskiy M.D. , Aaron Fleischman, Ph.D., D. Geoffrey Vince, Ph.D., Edward F. Plow1 and Olga Stenina-Adognravi The P387 Thrombospondin-4 Variant Promotes Accumulation of Macrophages in Atherosclerotic Lesions. *doi: 101101/666602* 2019.

17. Jasmine Gajeton IK, Revanth Yendamuri, Dmitriy Verbovetskiy, Amit Vasanji, Lidiya Sul, Olga Stenina-Adognravi miR-467 prevents inflammation and insulin resistance in response to hyperglycemia *doi: 101101/666545.* 2019.

18. Mosher DF, and Adams JC. Adhesion-modulating/matricellular ECM protein families: a structural, functional and evolutionary appraisal. *Matrix Biol.* 2012;31(3):155-61.

19. Adams JC. Matricellular Proteins: Functional Insights From Non-mammalian Animal Models. *Curr Top Dev Biol.* 2018;130:39-105.

20. Adams JC, and Lawler J. The thrombospondins. *Int J Biochem Cell Biol.* 2004;36(6):961-8.

21. Adams JC, and Lawler J. The thrombospondins. *Cold Spring Harb Perspect Biol.* 2011;3(10):a009712.

22. Adams JC. Thrombospondins: multifunctional regulators of cell interactions. *Annu Rev Cell Dev Biol.* 2001;17:25-51.

23. Paddock HN, Schultz GS, Baker HV, Varela JC, Beierle EA, Moldawer LL, et al. Analysis of gene expression patterns in human postburn hypertrophic scars. *J Burn Care Rehabil.* 2003;24(6):371-7.

24. Rysa J, Leskinen H, Ilves M, and Ruskoaho H. Distinct upregulation of extracellular matrix genes in transition from hypertrophy to hypertensive heart failure. *Hypertension.* 2005;45(5):927-33.

25. Pan B, Yu H, Park J, Yu YP, Luo ZD, and Hogan QH. Painful nerve injury upregulates thrombospondin-4 expression in dorsal root ganglia. *J Neurosci Res.* 2015;93(3):443-53.

26. Muppala S, Frolova E, Xiao R, Krukovets I, Yoon S, Hoppe G, et al. Proangiogenic Properties of Thrombospondin-4. *Arterioscler Thromb Vasc Biol.* 2015.

27. Crosby ND, and Winkelstein BA. Spinal Astrocytic Thrombospondin-4 Induced by Excitatory Neuronal Signaling Mediates Pain After Facet Capsule Injury. *Ann Biomed Eng.* 2016;44(11):3215-24.

28. Crosby ND, Zaucke F, Kras JV, Dong L, Luo ZD, and Winkelstein BA. Thrombospondin-4 and excitatory synaptogenesis promote spinal sensitization after painful mechanical joint injury. *Exp Neurol.* 2015;264:111-20.

29. Kim DS, Li KW, Boroujerdi A, Peter Yu Y, Zhou CY, Deng P, et al. Thrombospondin-4 contributes to spinal sensitization and neuropathic pain states. *J Neurosci.* 2012;32(26):8977-87.

30. Subramanian A, and Schilling TF. Thrombospondin-4 controls matrix assembly during development and repair of myotendinous junctions. *Elife.* 2014;3.

31. Amy EM, Song S, Kutasovic JR, Reid LE, Valle JM, Vargas AC, et al. Thrombospondin-4 expression is activated during the stromal response to invasive breast cancer. *Virchows Arch.* 2013;463(4):535-45.

32. Mustonen E, Aro J, Puhakka J, Ilves M, Soini Y, Leskinen H, et al. Thrombospondin-4 expression is rapidly upregulated by cardiac overload. *Biochem Biophys Res Commun.* 2008;373(2):186-91.

33. Stenina-Adognravi O, and Plow EF. Thrombospondin-4 in tissue remodeling. *Matrix Biol.* 2017.

34. Yang HJ, Ma SP, Ju F, Zhang YP, Li ZC, Zhang BB, et al. Thrombospondin-4 Promotes Neuronal Differentiation of NG2 Cells via the ERK/MAPK Pathway. *J Mol Neurosci.* 2016;60(4):517-24.

35. Frolova EG, Sopko N, Blech L, Popovic ZB, Li J, Vasanji A, et al. Thrombospondin-4 regulates fibrosis and remodeling of the myocardium in response to pressure overload. *FASEB J.* 2012;26(6):2363-73.

36. Arber S, and Caroni P. Thrombospondin-4, an extracellular matrix protein expressed in the developing and adult nervous system promotes neurite outgrowth. *J Cell Biol.* 1995;131(4):1083-94.

37. Cho JY, Lim JY, Cheong JH, Park YY, Yoon SL, Kim SM, et al. Gene expression signature-based prognostic risk score in gastric cancer. *Clin Cancer Res.* 2011;17(7):1850-7.

38. D'Errico M, de Rinaldis E, Blasi MF, Viti V, Falchetti M, Calcagnile A, et al. Genome-wide expression profile of sporadic gastric cancers with microsatellite instability. *Eur J Cancer.* 2009;45(3):461-9.

39. Singh D, Febbo PG, Ross K, Jackson DG, Manola J, Ladd C, et al. Gene expression correlates of clinical prostate cancer behavior. *Cancer Cell.* 2002;1(2):203-9.

40. Ma XJ, Wang Z, Ryan PD, Isakoff SJ, Barmettler A, Fuller A, et al. A two-gene expression ratio predicts clinical outcome in breast cancer patients treated with tamoxifen. *Cancer Cell.* 2004;5(6):607-16.

41. Curtis C, Shah SP, Chin SF, Turashvili G, Rueda OM, Dunning MJ, et al. The genomic and transcriptomic architecture of 2,000 breast tumours reveals novel subgroups. *Nature.* 2012;486(7403):346-52.

42. Lu X, Wang ZC, Iglehart JD, Zhang X, and Richardson AL. Predicting features of breast cancer with gene expression patterns. *Breast Cancer Res Treat.* 2008;108(2):191-201.

43. Muppala S, Xiao R, Krukovets I, Verbovetsky D, Yendamuri R, Habib N, et al. Thrombospondin-4 mediates TGF-beta-induced angiogenesis. *Oncogene.* 2017.

44. Ryu TY, Park J, and Scherer PE. Hyperglycemia as a risk factor for cancer progression. *Diabetes Metab J.* 2014;38(5):330-6.

45. Pisani P. Hyper-insulinaemia and cancer, meta-analyses of epidemiological studies. *Arch Physiol Biochem.* 2008;114(1):63-70.

46. Joslin EP, Lombard HL, Burrows RE, and Manning MD. Diabetes and cancer. *N Engl J Med.* 1959;260(10):486-8.

47. Giovannucci E, Harlan DM, Archer MC, Bergenstal RM, Gapstur SM, Habel LA, et al. Diabetes and cancer: a consensus report. *CA Cancer J Clin.* 2010;60(4):207-21.

48. Noto H, Tsujimoto T, Sasazuki T, and Noda M. Significantly increased risk of cancer in patients with diabetes mellitus: a systematic review and meta-analysis. *Endocr Pract.* 2011;17(4):616-28.

49. Barone BB, Yeh HC, Snyder CF, Peairs KS, Stein KB, Derr RL, et al. Long-term all-cause mortality in cancer patients with preexisting diabetes mellitus: a systematic review and meta-analysis. *JAMA.* 2008;300(23):2754-64.

50. Larsson SC, Bergkvist L, and Wolk A. Glycemic load, glycemic index and breast cancer risk in a prospective cohort of Swedish women. *Int J Cancer.* 2009;125(1):153-7.

51. Dong JY, and Qin LQ. Dietary glycemic index, glycemic load, and risk of breast cancer: meta-analysis of prospective cohort studies. *Breast Cancer Res Treat.* 2011;126(2):287-94.

52. Sieri S, Pala V, Brighenti F, Agnoli C, Grioni S, Berrino F, et al. High glycemic diet and breast cancer occurrence in the Italian EPIC cohort. *Nutr Metab Cardiovasc Dis.* 2013;23(7):628-34.

53. Turati F, Galeone C, Gandini S, Augustin LS, Jenkins DJ, Pelucchi C, et al. High glycemic index and glycemic load are associated with moderately increased cancer risk. *Mol Nutr Food Res.* 2015;59(7):1384-94.

54. Mullie P, Koechlin A, Boniol M, Autier P, and Boyle P. Relation between Breast Cancer and High Glycemic Index or Glycemic Load: A Meta-analysis of Prospective Cohort Studies. *Crit Rev Food Sci Nutr.* 2016;56(1):152-9.

55. Melkonian SC, Daniel CR, Ye Y, Pierzynski JA, Roth JA, and Wu X. Glycemic Index, Glycemic Load, and Lung Cancer Risk in Non-Hispanic Whites. *Cancer Epidemiol Biomarkers Prev.* 2016;25(3):532-9.

56. Hu J, La Vecchia C, Augustin LS, Negri E, de Groh M, Morrison H, et al. Glycemic index, glycemic load and cancer risk. *Ann Oncol.* 2013;24(1):245-51.

57. Hardin J, Cheng I, and Witte JS. Impact of consumption of vegetable, fruit, grain, and high glycemic index foods on aggressive prostate cancer risk. *Nutr Cancer.* 2011;63(6):860-72.

58. Nagle CM, Olsen CM, Ibiebele TI, Spurdle AB, Webb PM, Astralian National Endometrial Cancer Study G, et al. Glycemic index, glycemic load and endometrial cancer risk: results from the Australian National Endometrial Cancer study and an updated systematic review and meta-analysis. *Eur J Nutr.* 2013;52(2):705-15.

59. Larsson SC, Giovannucci EL, and Wolk A. Prospective Study of Glycemic Load, Glycemic Index, and Carbohydrate Intake in Relation to Risk of Biliary Tract Cancer. *Am J Gastroenterol.* 2016;111(6):891-6.

60. Sieri S, Krogh V, Agnoli C, Ricceri F, Palli D, Masala G, et al. Dietary glycemic index and glycemic load and risk of colorectal cancer: results from the EPIC-Italy study. *Int J Cancer.* 2015;136(12):2923-31.

61. Sieri S, Agnoli C, Pala V, Grioni S, Brighenti F, Pellegrini N, et al. Dietary glycemic index, glycemic load, and cancer risk: results from the EPIC-Italy study. *Sci Rep.* 2017;7(1):9757.

62. Abe H, Aida Y, Ishiguro H, Yoshizawa K, Miyazaki T, Itagaki M, et al. Alcohol, postprandial plasma glucose, and prognosis of hepatocellular carcinoma. *World J Gastroenterol.* 2013;19(1):78-85.

63. Keum N, Yuan C, Nishihara R, Zoltick E, Hamada T, Martinez Fernandez A, et al. Dietary glycemic and insulin scores and colorectal cancer survival by tumor molecular biomarkers. *Int J Cancer.* 2017;140(12):2648-56.

64. Dehghan M, Mente A, Zhang X, Swaminathan S, Li W, Mohan V, et al. Associations of fats and carbohydrate intake with cardiovascular disease and mortality in 18 countries from five continents (PURE): a prospective cohort study. *Lancet.* 2017;390(10107):2050-62.

65. Augustin LS, Kendall CW, Jenkins DJ, Willett WC, Astrup A, Barclay AW, et al. Glycemic index, glycemic load and glycemic response: An International Scientific Consensus Summit from the International Carbohydrate Quality Consortium (ICQC). *Nutr Metab Cardiovasc Dis.* 2015;25(9):795-815.

66. Augustin LS, Libra M, Crispo A, Grimaldi M, De Laurentiis M, Rinaldo M, et al. Low glycemic index diet, exercise and vitamin D to reduce breast cancer recurrence (DEDiCa): design of a clinical trial. *BMC Cancer.* 2017;17(1):69.

67. Hotamisligil GS. Inflammation and metabolic disorders. *Nature.* 2006;444(7121):860-7.

68. Lackey DE, and Olefsky JM. Regulation of metabolism by the innate immune system. *Nat Rev Endocrinol.* 2016;12(1):15-28.

69. Donath MY, and Shoelson SE. Type 2 diabetes as an inflammatory disease. *Nat Rev Immunol.* 2011;11(2):98-107.

70. Chawla A, Nguyen KD, and Goh YP. Macrophage-mediated inflammation in metabolic disease. *Nat Rev Immunol.* 2011;11(11):738-49.

71. Zhang X, Yang Y, and Zhao Y. Macrophage phenotype and its relationship with renal function in human diabetic nephropathy. *PLoS One.* 2019;14(9):e0221991.

72. Oh H, Park SH, Kang MK, Kim YH, Lee EJ, Kim DY, et al. Asaronic Acid Attenuates Macrophage Activation toward M1 Phenotype through Inhibition of NF-kappaB Pathway and JAK-STAT Signaling in Glucose-Loaded Murine Macrophages. *J Agric Food Chem.* 2019;67(36):10069-78.

73. Yuan Y, Chen Y, Peng T, Li L, Zhu W, Liu F, et al. Mitochondrial ROS-induced lysosomal dysfunction impairs autophagic flux and contributes to M1 macrophage polarization in a diabetic condition. *Clin Sci (Lond).* 2019;133(15):1759-77.

74. Pavlou S, Lindsay J, Ingram R, Xu H, and Chen M. Sustained high glucose exposure sensitizes macrophage responses to cytokine stimuli but reduces their phagocytic activity. *BMC Immunol.* 2018;19(1):24.

75. Loeys BL, Mortier G, and Dietz HC. Bone lessons from Marfan syndrome and related disorders: fibrillin, TGF-B and BMP at the balance of too long and too short. *Pediatr Endocrinol Rev.* 2013;10 Suppl 2:417-23.

76. Yokoyama H, and Deckert T. Central role of TGF-beta in the pathogenesis of diabetic nephropathy and macrovascular complications: a hypothesis. *Diabet Med.* 1996;13(4):313-20.

77. Hubmacher D, and Apte SS. The biology of the extracellular matrix: novel insights. *Curr Opin Rheumatol.* 2013;25(1):65-70.

78. Samarakoon R, Overstreet JM, and Higgins PJ. TGF-beta signaling in tissue fibrosis: redox controls, target genes and therapeutic opportunities. *Cell Signal.* 2013;25(1):264-8.

79. Lan HY, and Chung AC. TGF-beta/Smad signaling in kidney disease. *Semin Nephrol.* 2012;32(3):236-43.

80. Fernandez IE, and Eickelberg O. The impact of TGF-beta on lung fibrosis: from targeting to biomarkers. *Proc Am Thorac Soc.* 2012;9(3):111-6.

81. Weiss A, and Attisano L. The TGFbeta superfamily signaling pathway. *Wiley Interdiscip Rev Dev Biol.* 2013;2(1):47-63.

82. Katz LH, Li Y, Chen JS, Munoz NM, Majumdar A, Chen J, et al. Targeting TGF-beta signaling in cancer. *Expert Opin Ther Targets.* 2013;17(7):743-60.

83. Toma I, and McCaffrey TA. Transforming growth factor-beta and atherosclerosis: interwoven atherogenic and atheroprotective aspects. *Cell Tissue Res.* 2012;347(1):155-75.

84. Yang SN, Burch ML, Tannock LR, Evanko S, Osman N, and Little PJ. Transforming growth factor-beta regulation of proteoglycan synthesis in vascular smooth muscle: contribution to lipid binding and accelerated atherosclerosis in diabetes. *J Diabetes.* 2010;2(4):233-42.

85. Suriyamurthy S, Baker D, Ten Dijke P, and Iyengar PV. Epigenetic Reprogramming of TGF-beta Signaling in Breast Cancer. *Cancers (Basel).* 2019;11(5).

86. Khoshakhlagh M, Soleimani A, Binabaj MM, Avan A, Ferns GA, Khazaei M, et al. Therapeutic potential of pharmacological TGF-beta signaling pathway inhibitors in the pathogenesis of breast cancer. *Biochem Pharmacol.* 2019;164:17-22.

87. Dabir P, Marinic TE, Krukovets I, and Stenina OI. Aryl hydrocarbon receptor is activated by glucose and regulates the thrombospondin-1 gene promoter in endothelial cells. *Circ Res.* 2008;102(12):1558-65.

88. Stenina OI, Ustinov V, Krukovets I, Marinic T, Topol EJ, and Plow EF. Polymorphisms A387P in thrombospondin-4 and N700S in thrombospondin-1 perturb calcium binding sites. *FASEB J.* 2005;19(13):1893-5.

89. Stenina OI, Desai SY, Krukovets I, Kight K, Janigro D, Topol EJ, et al. Thrombospondin-4 and its variants: expression and differential effects on endothelial cells. *Circulation.* 2003;108(12):1514-9.

90. Frolova EG, Drazba J, Krukovets I, Kostenko V, Blech L, Harry C, et al. Control of organization and function of muscle and tendon by thrombospondin-4. *Matrix Biol.* 2014;37:35-48.

91. Chopra M, and Schrenk D. Dioxin toxicity, aryl hydrocarbon receptor signaling, and apoptosis-persistent pollutants affect programmed cell death. *Crit Rev Toxicol.* 2011;41(4):292-320.

92. LaValley DJ, Zanotelli MR, Bordeleau F, Wang W, Schwager SC, and Reinhart-King CA. Matrix Stiffness Enhances VEGFR-2 Internalization, Signaling, and Proliferation in Endothelial Cells. *Converg Sci Phys Oncol.* 2017;3.

93. Krukovets I, Legerski M, Sul P, and Stenina-Adognravi O. Inhibition of hyperglycemia-induced angiogenesis and breast cancer tumor growth by systemic injection of microRNA-467 antagonist. *FASEB J.* 2015.

94. Bhattacharyya S, Sul K, Krukovets I, Nestor C, Li J, and Adognravi OS. Novel tissue-specific mechanism of regulation of angiogenesis and cancer growth in response to hyperglycemia. *J Am Heart Assoc.* 2012;1(6):e005967.

A

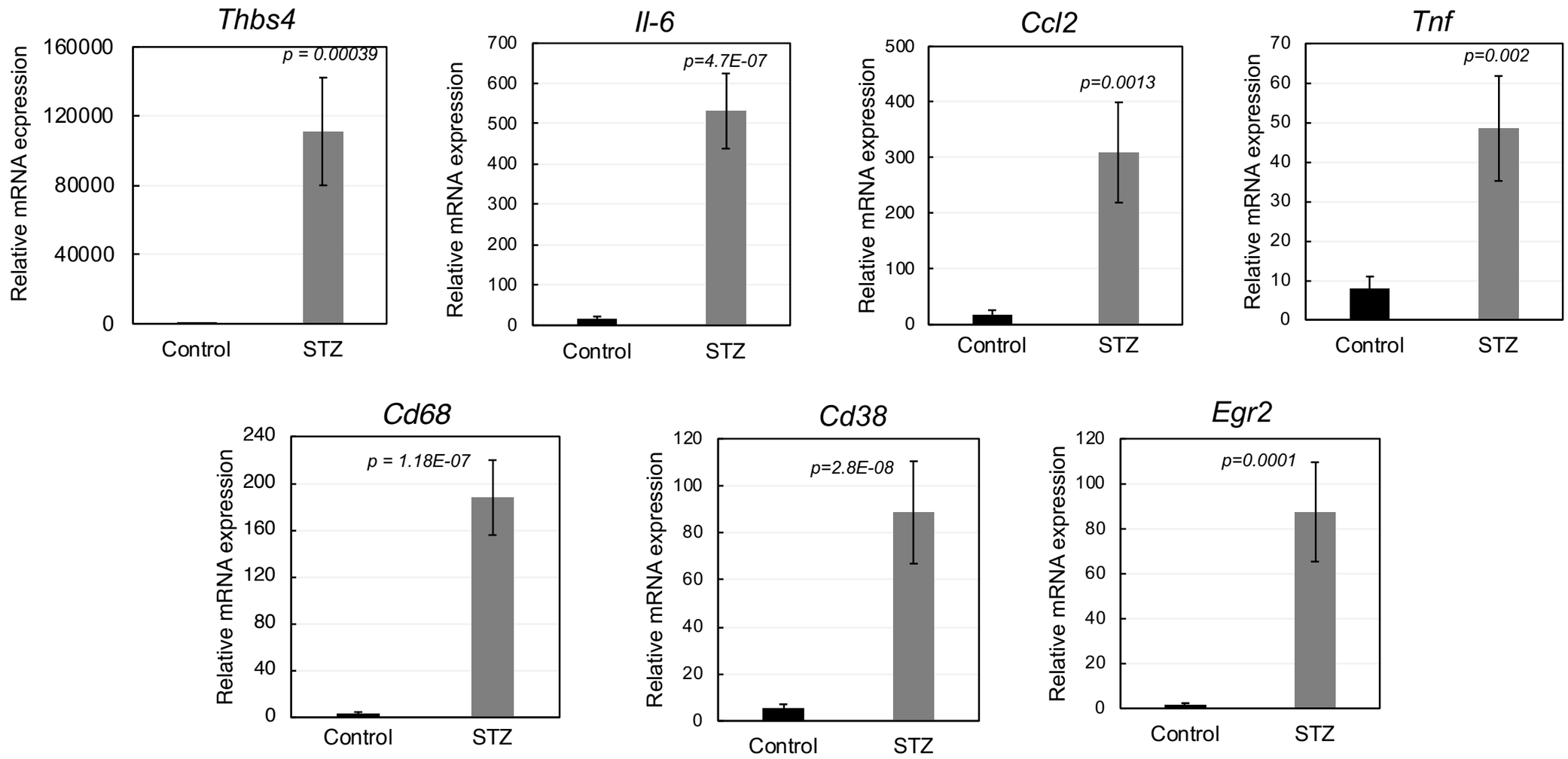
Thbs4
Relative mRNA ecpression
p = 0.00039
Control
STZ
Il-6
Relative mRNA expression
p=4.7E-07
Control
STZ
Ccl2
Relative mRNA expression
p=0.0013
Control
STZ
Tnf
Relative mRNA expression
p=0.002
Control
STZ
Cd68
Relative mRNA expression
p = 1.18E-07
Control
STZ
Cd38
Relative mRNA expression
p=2.8E-08
Control
STZ
Egr2
Relative mRNA expression
p=0.0001
Control
STZ

B

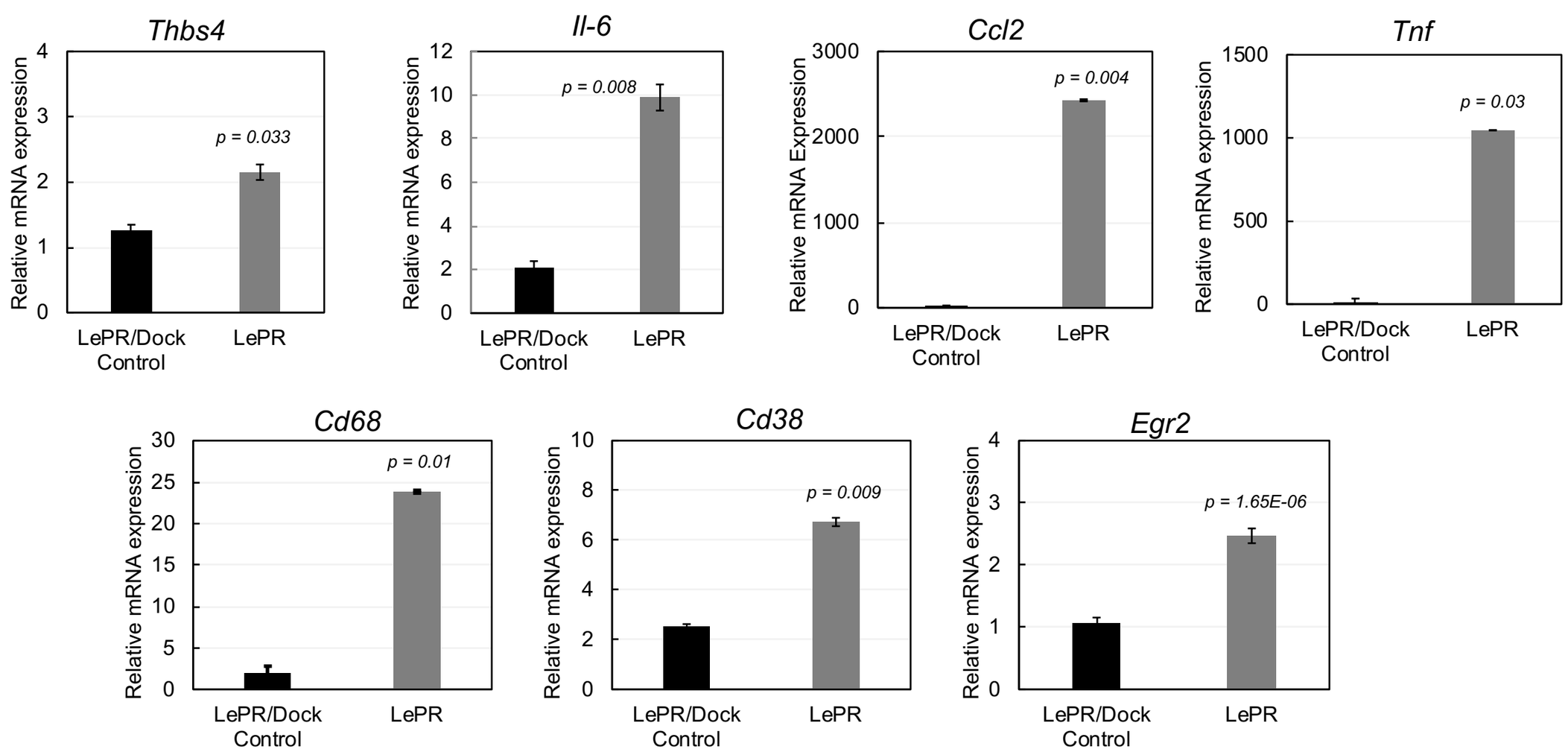
Thbs4
Relative mRNA expression
p = 0.033
LePR/Dock Control
LePR
Il-6
Relative mRNA expression
p = 0.008
LePR/Dock Control
LePR
Ccl2
Relative mRNA Expression
p = 0.004
LePR/Dock Control
LePR
Tnf
Relative mRNA expression
p = 0.03
LePR/Dock Control
LePR
Cd68
Relative mRNA expression
p = 0.01
LePR/Dock Control
LePR
Cd38
Relative mRNA expression
p = 0.009
LePR/Dock Control
LePR
Egr2
Relative mRNA expression
p = 1.65E-06
LePR/Dock Control
LePR

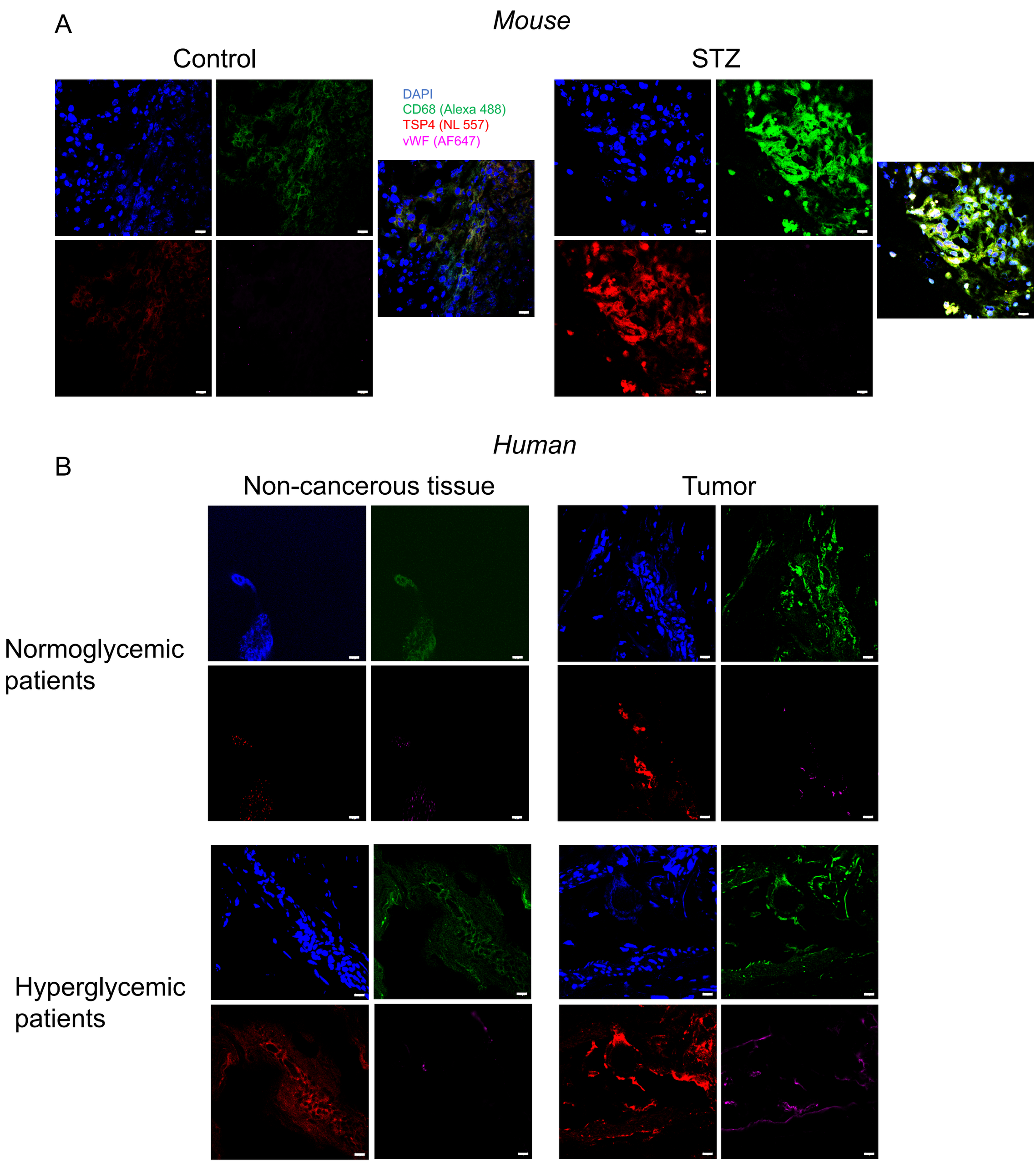
A
Mouse
Control
STZ
DAPI
CD68 (Alexa 488)
TSP4 (NL 557)
vWF (AF647)
B
Human
Non-cancerous tissue
Tumor
Normoglycemic patients
Hyperglycemic patients

A

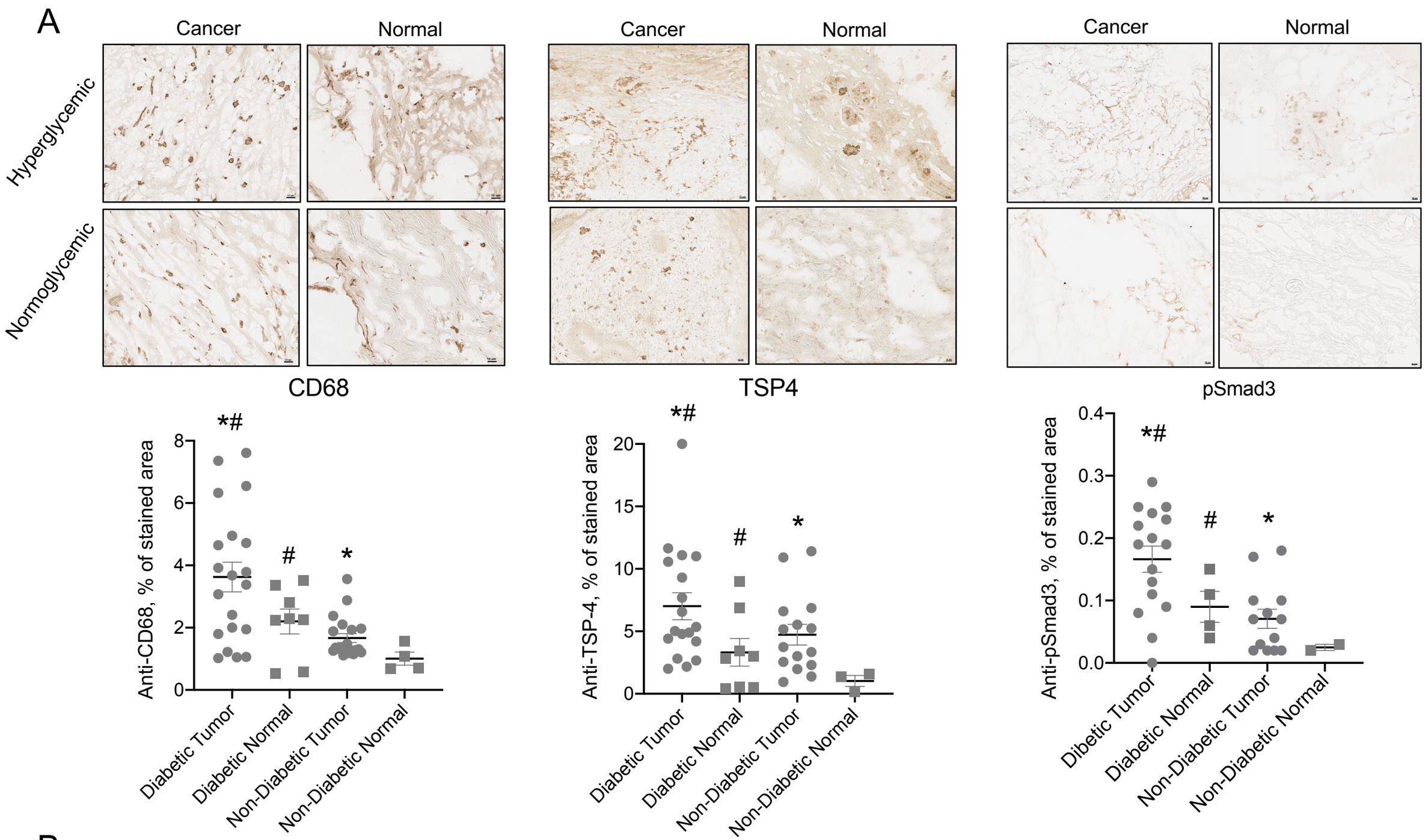
Cancer
Normal
Hyperglycemic
Normoglycemic
CD68
Anti-CD68, % of stained area
TSP4
Anti-TSP-4, % of stained area
pSmad3
Anti-pSmad3, % of stained area
*#
#
*
Diabetic Tumor
Diabetic Normal
Non-Diabetic Tumor
Non-Diabetic Normal
Dibetic Tumor

B

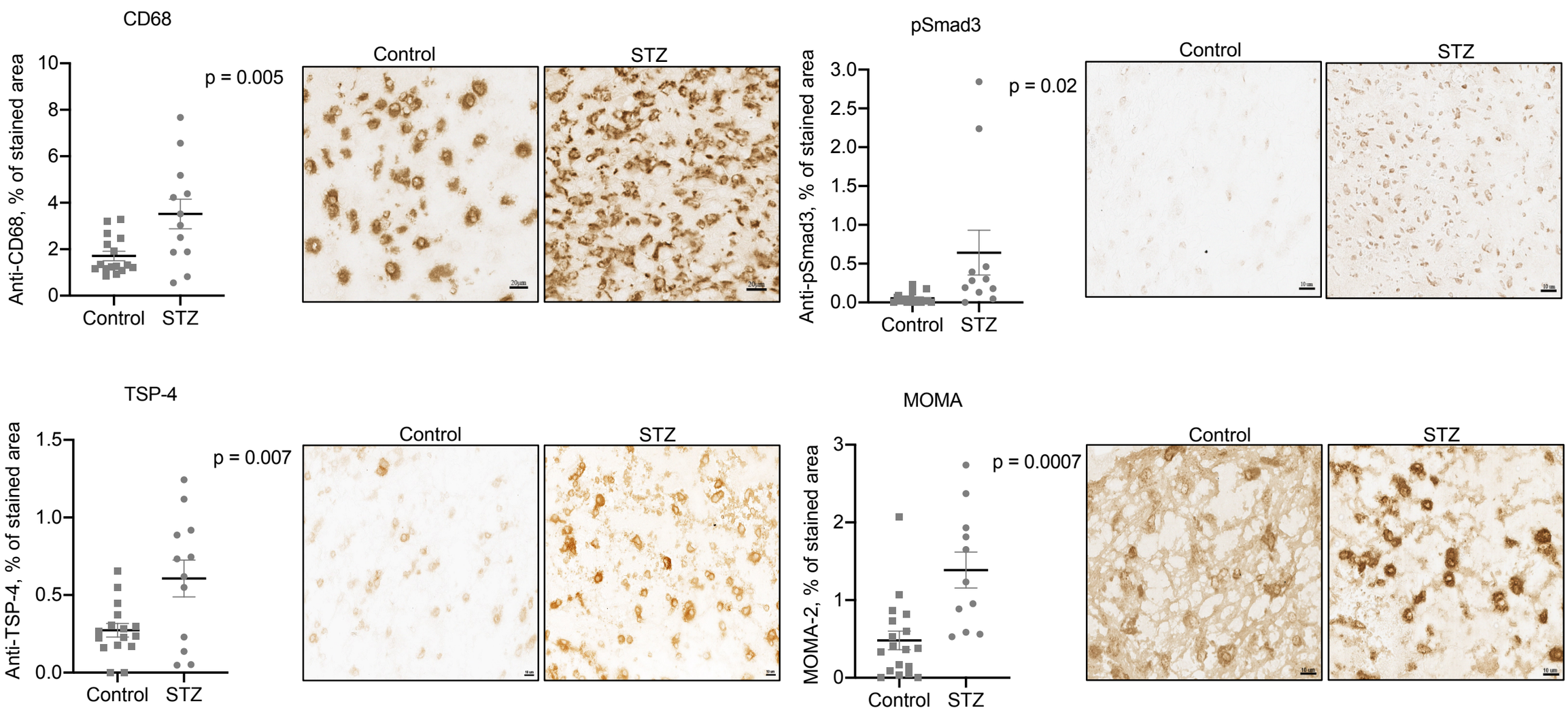
CD68
Anti-CD68, % of stained area
p = 0.005
Control
STZ
pSmad3
Anti-pSmad3, % of stained area
p = 0.02
TSP-4
Anti-TSP-4, % of stained area
p = 0.007
MOMA
MOMA-2, % of stained area
p = 0.0007

A

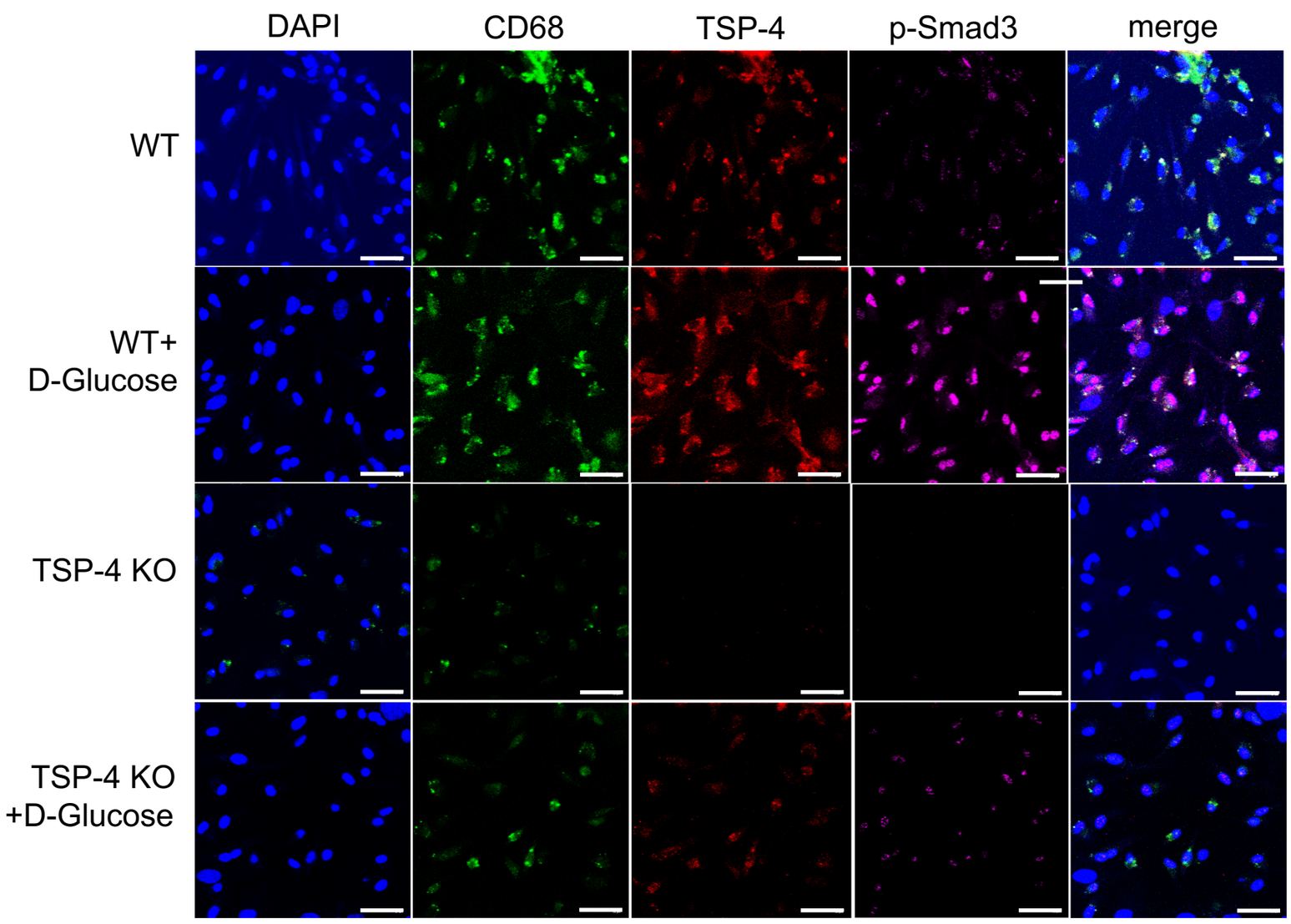

DAPI
CD68 (AF 493)
TSP-4 (NL 557)
p-Smad3 (AF647)

B

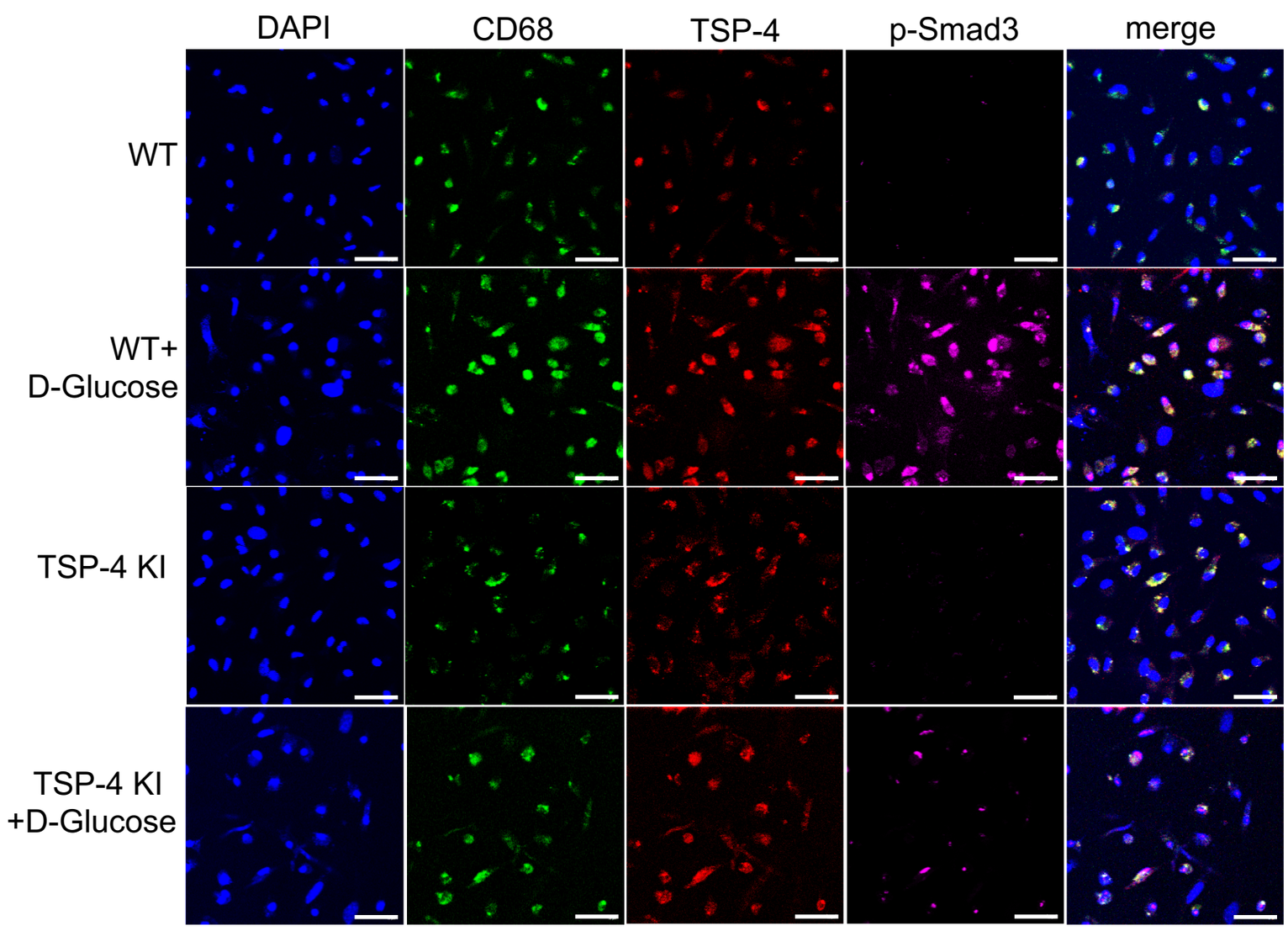

A

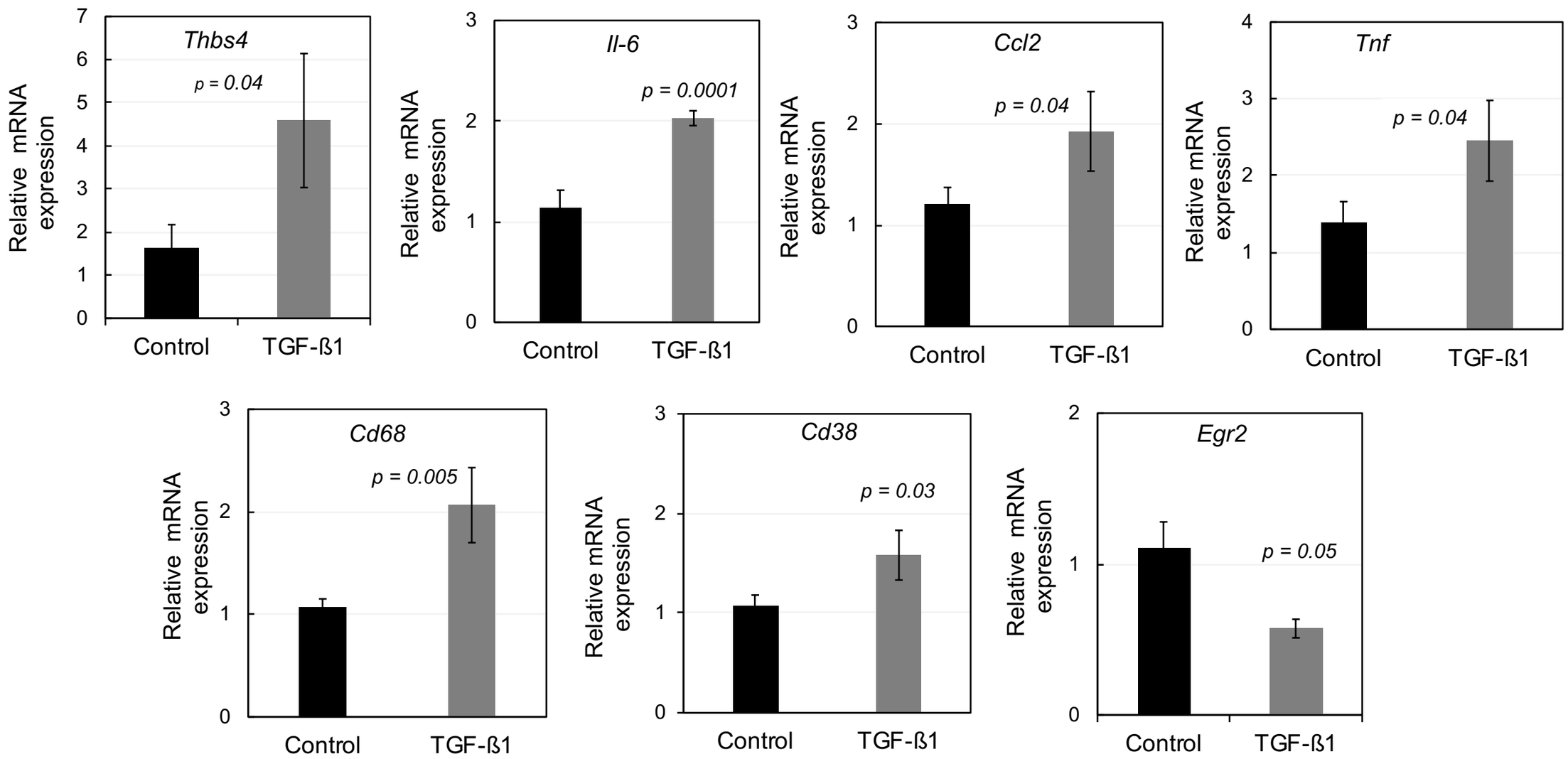
Thbs4
p = 0.04
Il-6
p = 0.0001
Ccl2
p = 0.04
Tnf
p = 0.04
Cd68
p = 0.005
Cd38
p = 0.03
Egr2
p = 0.05
Relative mRNA expression
Control
TGF-ß1

B

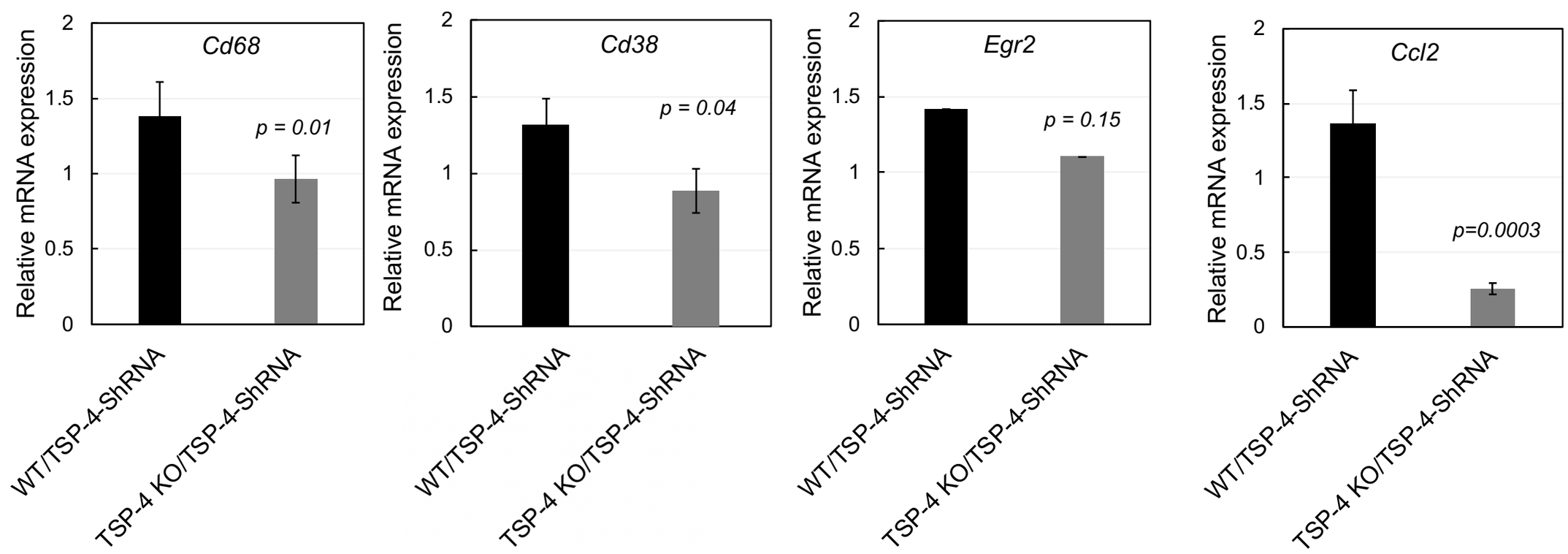
Cd68
p = 0.01
Cd38
p = 0.04
Egr2
p = 0.15
Ccl2
p=0.0003
Relative mRNA expression
WT/TSP-4-ShRNA
TSP-4 KO/TSP-4-ShRNA

A

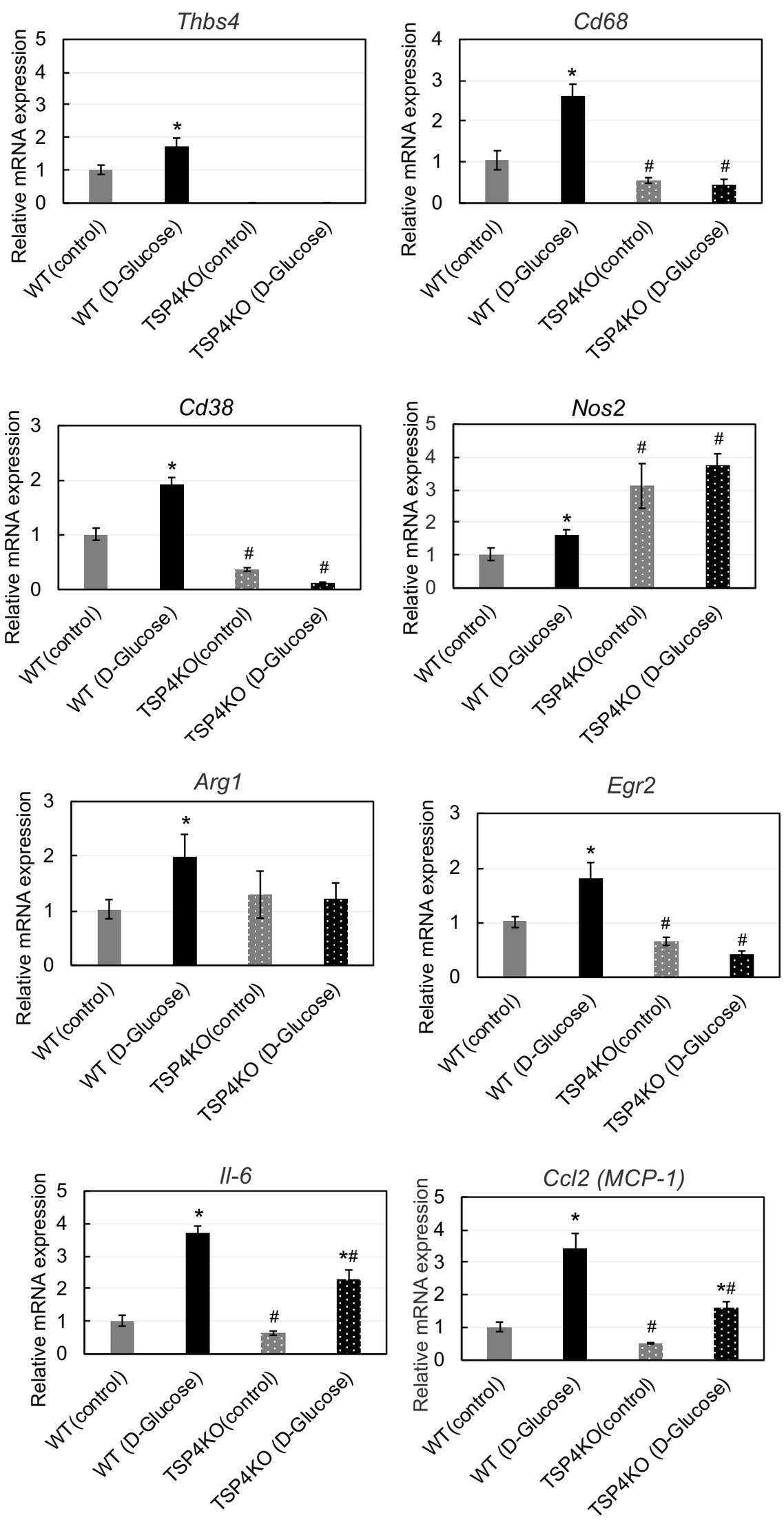
Thbs4
Cd68
Cd38
Nos2
Arg1
Egr2
Il-6
Ccl2 (MCP-1)
Tnf
Relative mRNA expression
WT (control)
WT (D-Glucose)
TSP4KO(control)
TSP4KO (D-Glucose)

B

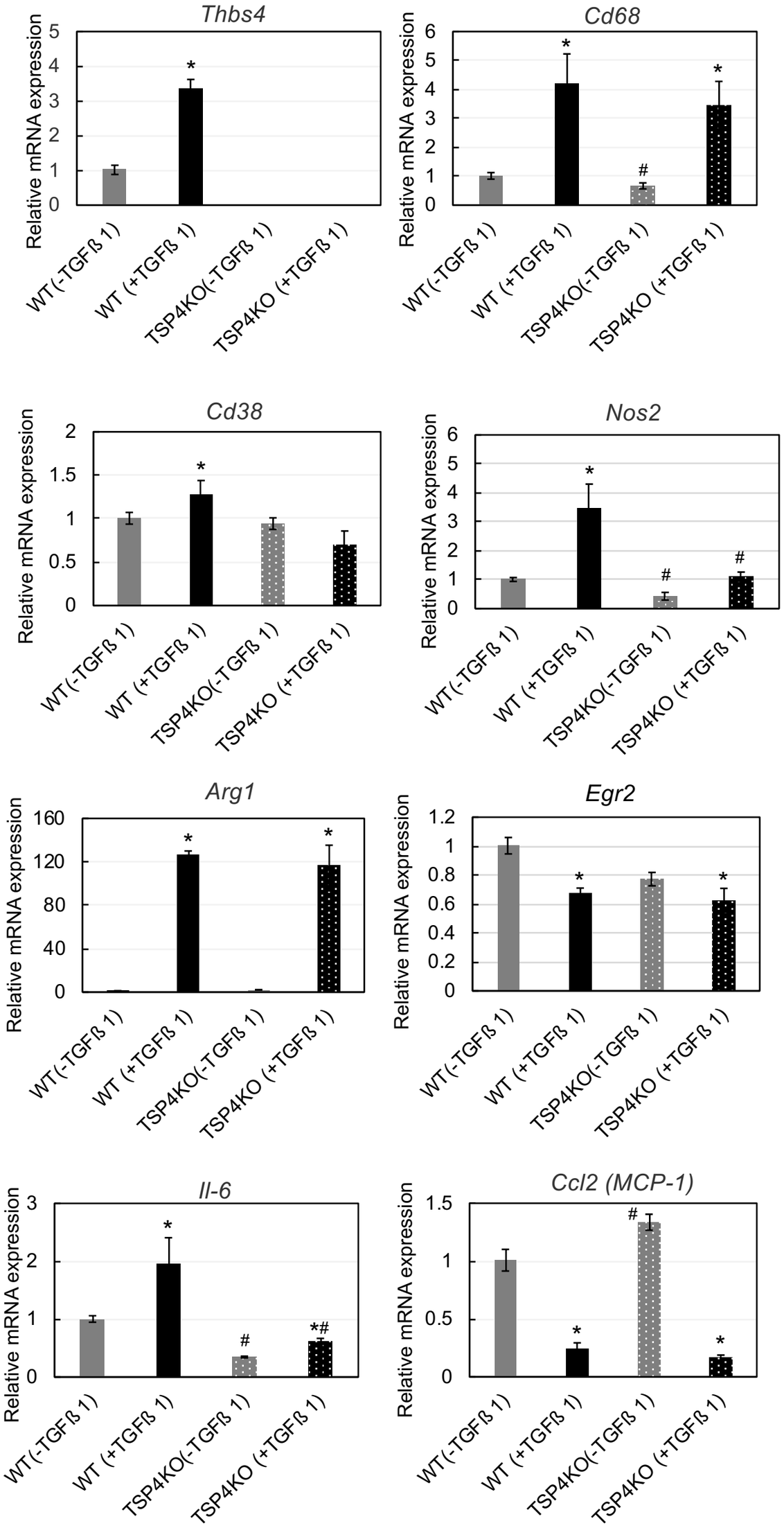
Thbs4
Cd68
Cd38
Nos2
Arg1
Egr2
Il-6
Ccl2 (MCP-1)
Tnf
Relative mRNA expression
WT (-TGFß 1)
WT (+TGFß 1)
TSP4KO(-TGFß 1)
TSP4KO (+TGFß 1)

A

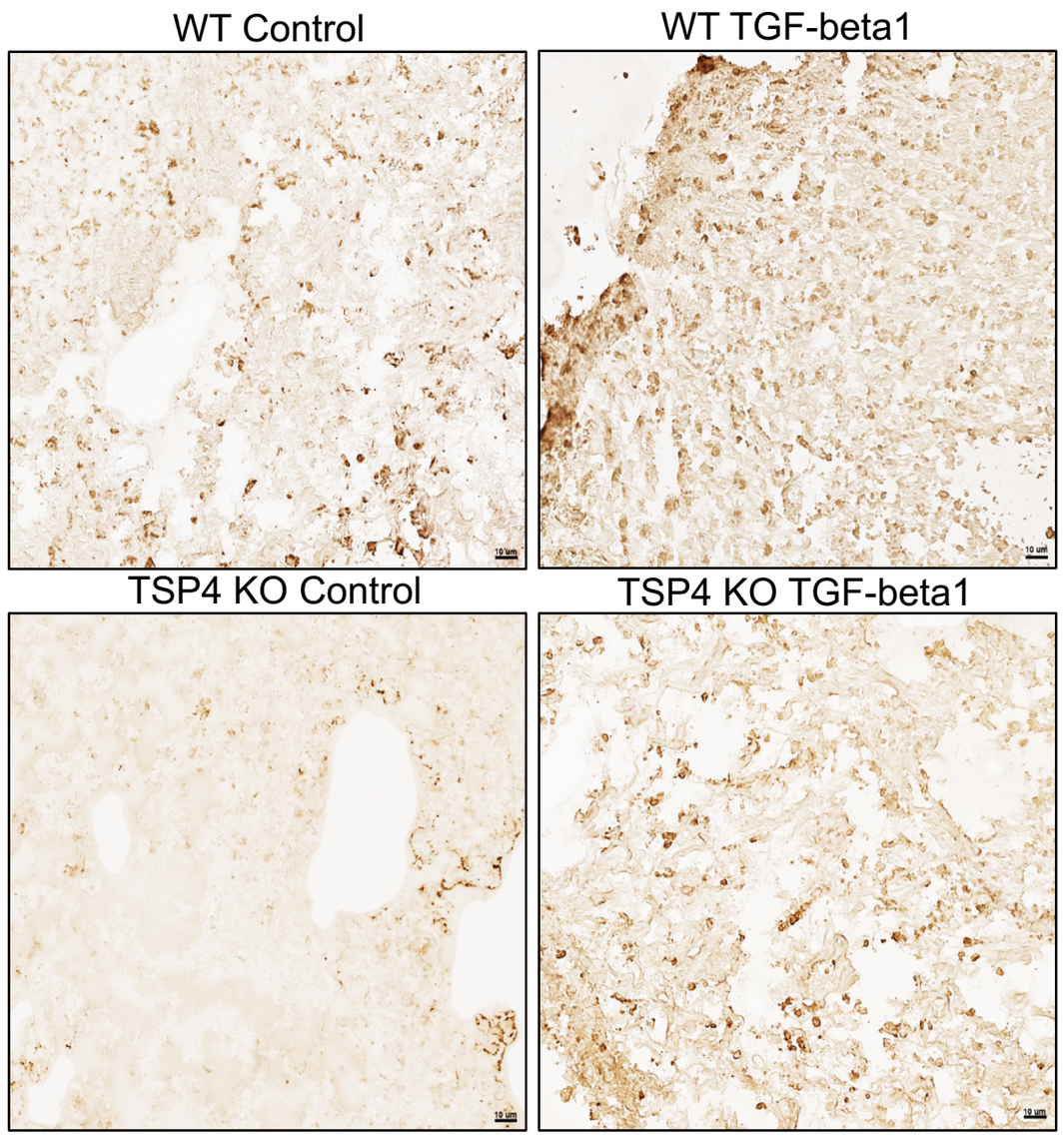
WT Control
WT TGF-beta1
TSP4 KO Control
TSP4 KO TGF-beta1

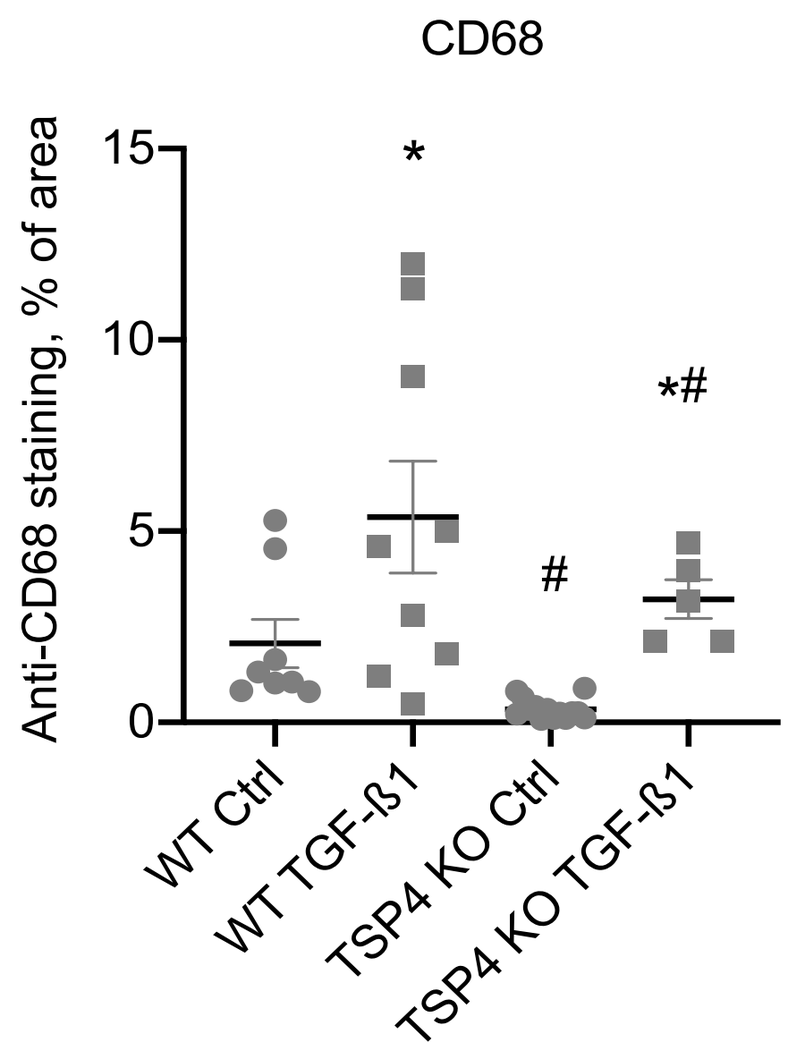
CD68
Anti-CD68 staining, % of area
15
10
5
0
*
*#
#
WT Ctrl
WT TGF-ß1
TSP4 KO Ctrl
TSP4 KO TGF-ß1

B

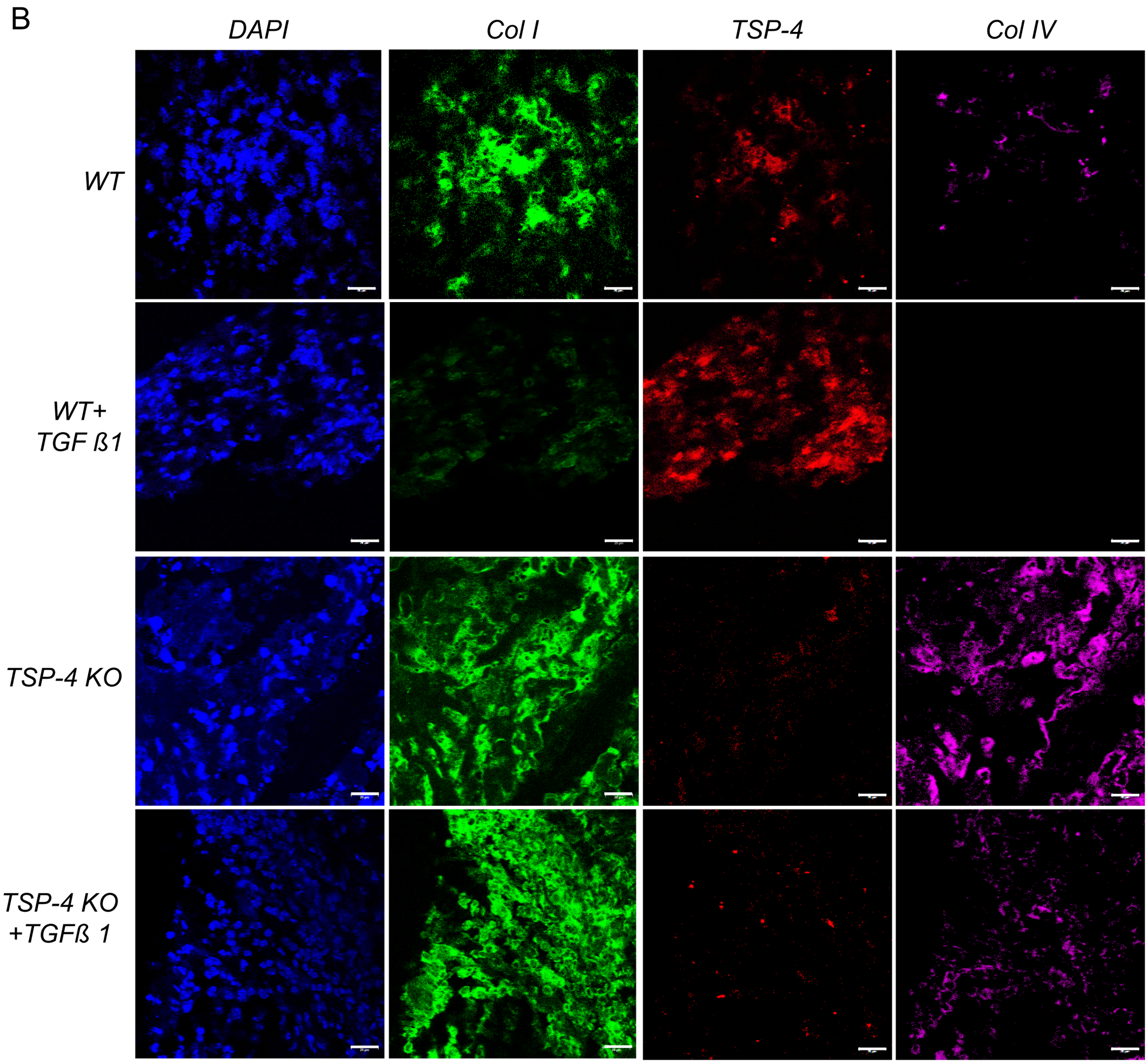
DAPI
Col I
TSP-4
Col IV
WT
WT+
TGF ß1
TSP-4 KO
TSP-4 KO
+TGFß 1